FINAL TECHNICAL REPORT

For U.S. Geological Survey

SEISMIC RESPONSE OF FOUNDATIONS FROM PILE-SYSTEM AND ADJACENT DOWNHOLE-ARRAY EARTHQUAKE RECORDS

Award Number: G13AP00050

Project Title: Seismic Response of Foundations from Pile-System and Adjacent Downhole-Array Earthquake Records

Principal Investigator: Ahmed Elgamal

Department of Structural Engineering

University of California, San Diego

SME building, MC-0085

9500 Gilman Drive

La Jolla, CA 92093-0085

Tel. (858) 822-1075, Fax. (858) 534-1310

Email: elgamal@ucsd.edu

Graduate Student Researcher: Ning Wang

Department of Structural Engineering

University of California, San Diego

Term covered: July 2013 - December 2014

Date: 22 January 2015

Acknowledgements

The research presented in this report was funded by the U.S. Geological Survey award No. G13AP00050. Partial additional funding was provided by the Pacific Earthquake Engineering Research (PEER) Center. We greatly appreciate the advice and assistance provided by Mr. Tom Shantz of Caltrans, and by Mr. Tony Shakal and Dr. Moh Huang of the CGS SMIP.

Contents

1 Introduction 7
2 Eureka Geotechnical Downhole Array Data Analysis 8
2.1 Introduction 8
2.2 Site Description and General Information 8
2.2.1 Geotechnical Downhole Array at Eureka Station 89734 8
2.2.2 Available Earthquake Records 9
2.2.3 Site Description 9
2.3 Evaluation of Strong Motion Data 10
2.3.1 Recorded Time Histories 10
2.3.2 Cross Correlation Analysis 10
2.3.3 Site Resonant Characteristics 11
2.4 Summary and Conclusions 12
3 Recorded Seismic Response of the Samoa Channel Bridge System 21
3.1 Strong-Motion Instrumentations at the Samoa Channel Bridge and Adjacent Downhole Array 21
3.1.1 General Bridge Information 21
3.1.2 Original Construction and Seismic Retrofit 22
3.1.3 Instrumentations of the Samoa Channel Bridge 22
3.1.4 The Adjacent Eureka Geotechnical Array 23
3.1.5 Recorded Earthquake Motions 24
3.2 Evaluation of the Earthquake Records 24
3.2.1 Ground Motions at the Bridge and Adjacent Downhole Sites 25
3.2.2 Seismic Response along the Bridge Deck 26
3.2.3 Seismic Response of Pier S-8 27
3.2.4 Abutment and Bridge Response along Mud-line 28
3.3 System Identification for the Ground-Foundation-Bridge System 29
3.4 Discussion and Conclusions 30
4 Numerical Analysis of the Samoa Channel Bridge System 49
4.1 Introduction 49
4.2 General Bridge Information 49
4.2.1 Original Bridge Foundation 49
4.2.2 Site Description 50
4.3 Insights from the FE Analysis of Pier S-8 50

4.3.1 Finite Element Modeling 50
4.3.2 Calibration of the Pier Column Model at Pier S-8 52
4.3.3 Calibration of the Pile Foundation Model at Pier S-8 52
4.4 Conclusions 53
5 Recorded Seismic Response and Numerical Analysis of the Eureka Channel Bridge 59
5.1 Introduction 59
5.2 General Bridge Information 60
5.2.1 The Bridge Description 60
5.2.2 Site Description 61
5.2.3 Seismic Retrofit Effort 61
5.3 Strong-Motion Instrumentations at the Eureka Channel Bridge 62
5.3.1 Instrumentations of the Eureka Channel Bridge 62
5.3.2 Recorded Earthquake Motions 63
5.4 Evaluation of Earthquake Records 63
5.4.1 Ground Motions at the Bridge and Adjacent Downhole Sites 63
5.4.2 Seismic Response along the Bridge Deck 65
5.4.3 Seismic Response of Pier E-7 65
5.4.4 Abutment and Bridge Response along Mudline 66
5.5 System Identification for the Ground-Foundation-Bridge System 67
5.6 Finite Element Analysis 67
5.6.1 Finite Element Modeling 67
5.6.2 Structural Modeling of the Column at Pier E-7 68
5.6.3 Structural Modeling of the Pile Foundation below Pier E-7 69
5.6.4 Modeling of Base Springs 70
5.7 Conclusions 70
6 Conclusions 88
6.1 Strong Motion Data Analysis 88
6.2 Numerical Modeling of Ground-Foundation-Structure system 89

SEISMIC RESPONSE OF FOUNDATIONS FROM PILE-SYSTEM AND ADJACENT DOWNHOLE-ARRAY EARTHQUAKE RECORDS

Abstract

The January 9, 2010 Eureka Ferndale event has resulted in valuable earthquake records from instrumented foundation piles and a nearby free-field downhole geotechnical array. Data from an instrumented pile within a foundation pile-group in two different Bridges (the Eureka-Samoa Channel and Eureka- Eureka Channel bridges) are part of the overall recorded ground and bridge responses at these locations.

With this recorded moderate but substantial level of earthquake excitation, an ensemble of recorded low to moderate shaking events at these two sites (and the nearby downhole array) is available to provide a unique opportunity for documenting and analyzing this important ground-pile-system response mechanism.

In this research project, recorded seismic motions of the deep foundations, the bridge structures and an adjacent downhole-array (within an overall framework) were employed to fully analyze the ground-pile system response case history. Linear and nonlinear response of the ground and the bridge are assessed using system identification techniques. Finite Element (FE) models of the mid-span bridge piers are developed and calibrated. Methodologies combining numerical modeling with insights gained from the strong motion sensor records are investigated to capture the essential structure-foundation-ground system-response mechanisms. Focus is placed on the evaluation of dynamic properties and validation of the bridge FE models based on the recorded earthquake response. The important ground-pile-system response mechanisms are

explored in much detail. In general, the results of this research are of significant consequence to the current state of knowledge in seismic pile-ground analysis and design.

1 Introduction

Elucidation of the seismic response of ground-foundation systems, directly from recorded seismic records, is a major (and currently unique) opportunity, shedding light on actual full-scale behavior (to augment our analyses and analytical/experimental understandings). The objective of the research presented in this report is to further advance the procedures for numerical simulation of soil-foundation-structure systems by conducting the following studies:

- Strong motion data of two instrumented bridges in Eureka, CA and one adjacent downhole array collected through the joint efforts of the California Strong Motion Instrumentation Program (CSMIP) and the California Department of Transportation (Caltrans) are documented and analyzed. Response of the embedded instrumentation inside the piles are compared with all ground surface records (including the free-field, motion at different pile caps and at the abutments);
- Seismic response of the downhole site and the two instrumented bridges during the observed earthquake events is evaluated using system identification techiniques;
- FE models for the two bridge piers (Samoa Channel Bridge Pier S-8 and Eureka Channel Bridge Pier E-7) are developed and calibrated;
- The corresponding exerted lateral pile-group resistance are documented to explore the salient characteristics of the ground-foundation system.

2 Eureka Geotechnical Downhole Array Data Analysis

2.1 Introduction

Geotechnical downhole-arrays monitoring seismic response in near-surface strata provide valuable information on local soil dynamic characteristics. In this section, geotechnical downhole array records at the Eureka, California site are employed to examine the linear/nonlinear ground response. This downhole array was installed by CSMIP in cooperation with Caltrans in 1995 (Graizer et al. 2000). Cross-correlation analyses and spectral system identification are performed to evaluate the average shear wave velocities and site resonant frequencies. Nonlinear site response during the moderate shaking event of Ferndale Earthquake (Mw 6.5) on Jan 9, 2010 was observed. In addition, a 1-D numerical model of the site is developed using the finite element (FE) program - Cyclic1D (Elgamal et al. 2006). This FE model is calibrated using the identified site characteristics. Computational simulation results are presented, discussed, and compared to the recorded seismic site response.

2.2 Site Description and General Information

2.2.1 Geotechnical Downhole Array at Eureka Station 89734

The Eureka Geotechnical Downhole Array (GDA, CSMIP Station 89734) located between the Samoa Channel Bridge and the Middle Channel Bridge (Figure 2.1) was instrumented through the joint efforts of CSMIP and Caltrans in 1995. Horizontal and vertical motion sensor layouts as well as shear/pressure wave velocity profiles of the underlying soil from geophysical test are shown in Figure 2.2 and Figure 2.3. This downhole array consists of 15 accelerometers at five different depths (ground surface, 19 m, 33 m, 56 m, and 136 m) oriented

in the north-south (NS), east-west (EW) and vertical directions. Elevation of the ground surface sensors is +1 m with respect to the MSL (Mean Sea Level, personal communication with USGS). Due to the grade in the immediate area, elevation of the ground at the location of the downhole sensors near the road is estimated to be +3 m with respect to MSL (Figure 2.2). Therefore, elevations for the downhole sensors are +1 m, -16 m, -30 m, -53 m and -133 m all referenced to MSL.

2.2.2 Available Earthquake Records

A total of ten earthquakes (Table 2.1) have been recorded in the period of March 2000 through October 2012 with magnitudes from 4.1 M_w to 7.2 M_L (M_w: regional moment magnitude and M_L: local magnitude). Notable is the 2010 Ferndale Earthquake (hereafter, referred to as "the moderate event") causing a peak ground motion of around 20% g at this site. This M_w 6.5 Ferndale earthquake occurred off the coast of the Humboldt Bay Area, California is the largest earthquake in Humboldt County since the Crescent City Offshore Earthquake in 2005 (with an epicenter that is farther away 153.8 m) from the downhole site.

2.2.3 Site Description

A deep soft alluvium geological profile with high water table exists at this location. Subsurface data from a boring test conducted by of the Caltrans show 10 m of very soft clayey silt underlain by slightly compact gray materials. The very dense soil layer is approximately 22 m below the ground surface (Figure 2.4).

Shear velocity (V_s) and pressure wave velocity (V_p) profiles down to a depth of 225 meters are provided by USGS (Figure 2.3). The shear wave velocities are about 158 m/s -230 m/s in the upper 20 meters, and lie in the range of 210 m/s to 460 m/s at the depths of 20 to 60

meters. Bedrock appears to be at a depth of 220 m where the shear wave velocity reaches 870 m/s. The calculated Poisson's ratio at the elevation of each downhole sensor generally indicating saturated soil conditions (Wang 2015).

2.3 Evaluation of Strong Motion Data

2.3.1 Recorded Time Histories

Sensors of the geotechnical downhole array installed at different depths provide acceleration time histories which can be used to study the local soil profile. The recorded time histories along the depths during the moderate earthquake (shown in Wang 2015) indicate that the ground movement was amplified from 3.71 cm at the depth of 136 m (Elev. = -133 m) to 9.98 cm at the surface (Elev. = +1 m) (an increase of 1.7 fold).

2.3.2 Cross Correlation Analysis

In this report, seismic shear waves are assumed to propagate vertically. Cross correlation analysis is performed to estimate time needed for shear waves to propagate upwards (incident waves) or downwards (reflected waves) between downhole stations in the north-south and east-west directions (details in Wang 2015). Nonlinearity of the site seismic response was particularly evident during the moderate event. Lower average shear wave velocities are obtained when the strong motion phase of the moderate 2010 Ferndale Earthquake is included. The estimated average shear wave velocity decreased during the 30 s - 35 s time window (V_S = 121.4 m/s in Table 2.2 and Table 2.3), leading to a reduction of shear modulus of about 60% for the topmost stratum (elevation of +1 m to -16 m). Average shear strain (Elgamal et al. 1995; Zeghal et al. 1995) during this strong motion time window reached a maximum of about 0.09% (Figure 2.5).

The estimated shear modulus (40 percent of the initial shear modulus at shear strain of 0.09%) agrees with the shear modulus degradation curves for sand after Seed and Idriss (1970) as well as after EPRI (1993), which is in a range of 27% -38% for depths ranging from 0 m to 15.24 m (Figure 2.6).

Overall, the geophysical measurements of shear wave velocity are within this estimated range as shown in Figure 2.7. Since only slightly difference is observed for shear wave velocities in the NS and in EW directions, no appreciable azimuthal anisotropy of the soil at this location is evident.

2.3.3 Site Resonant Characteristics

Resonant frequency analyses utilizing a fast Fourier transform algorithm for the topmost stratum are conducted in two directions (Wang 2015). Fourier Spectral ratio analyses based on selected earthquakes are shown in Table 2.2 and Table 2.3 where the predicted first resonance is in a range of 2.30-3.11 Hz for the low amplitude shaking events. The identified first resonant frequency is in the neighborhood of that estimated by the simple constant shear modulus resonant shear beam formula of $f_1 = V_s/(4H)$ = 2.27-2.78 Hz (where f_1 is first resonant frequency, and H is vertical distance between sensors). The predominant frequency of the moderate event shifted to a lower frequency of f_1 = 1.90 Hz ($f_1 = V_s/(4H)$ =1.79 Hz). Such shift reflects a decrease in modulus and indicates the nonlinearity of soil during this moderate shaking event (Elgamal et al. 1995; Elgamal et al. 1996).

Fourier spectral ratios between the top two stations (elevation of +1 m to -16 m) were computed with a 5-second time window for the moderate event (Wang 2015). During the early and late parts of the recorded motion, natural frequency reached as much as 2.60 Hz. During the strong motion phase (30 s - 35 s), a lower natural frequency (decrease of soil stiffness) is noted

(~1.8 Hz). For the low amplitude earthquake, resonant frequency between the top two sensors is quite stable. The reduction of resonant frequency due to the softening of the soil domain during the moderate shaking event may contribute to changes in the adjacent bridge foundation stiffness.

In order to verify the estimated shear wave velocity, FE program Cyclic1D is employed to model the ground motion. A shear-beam model with calibrated soil properties is developed to represent the site dynamic response. NS and EW seismic motions measured by downhole array at the elevation of -53 m are considered as the input excitation. It is seen that there is a good degree of agreement between the time domain records and computed response. Simulation results and estimates of the soil shear modulus and Raleigh damping ratio are presented in details in Wang (2015).

2.4 Summary and Conclusions

Based on recorded ground motions of a five-level downhole array located in the Eureka area, soil shear wave velocities were back-calculated and site resonant frequencies are estimated. The identified site seismic characteristics are found to be in reasonable agreement with earlier in-situ measured data. Both shear-wave analysis and resonant frequency analysis illustrate nonlinear dynamic soil behavior during the moderate 2010 Ferndale earthquake event. A shear-beam model was developed using Cyclic1D to simulate site seismic response. Computed site response is comparable to the actual recorded counterpart.

Table 2.1: Earthquakes recorded by station 89734 Eureka Geotechnical Array

Earthquake	**Date**	**Record length (s)**	**Magnitude**	**Epic. Dist. (km)**	**Horiz PGA** (g)**	
					NS	**EW**
Ferndale [a]	01/09/2010	90.0	6.5 (M_w)	54.0	0.195	0.143
Trinidad	06/24/2007	60.0	5.1 (M_L)	64.3	0.055	-----*
Weitchpec	02/13/2012	60.0	5.6 (M_w)	47.9	0.029	0.038
Ferndale [b]	02/04/2010	66.0	5.9 (M_w)	77.6	0.025	0.021
Bluelake	10/21/2012	56.0	3.5 (M_L)	22.2	0.013	0.008
Eureka Offshore	09/22/2000	40.0	4.4 (M_L)	24.4	0.011	0.010
Ferndale [c]	02/26/2007	59.0	5.4 (M_L)	62.6	0.007	0.010
Crescent City	06/14/2005	104.0	7.2 (M_L)	153.8	0.006	0.008
Ferndale Offshore	12/27/2000	37.0	4.1 (M_w)	46.4	0.007	0.005
Cape Mendocino	03/16/2000	75.0	5.6 (M_w)	102.6	0.004	0.004

* malfunction of accelerometer at the ground surface
** PGA = Peak Ground Acceleration
Ferndale [a]: Ferndale Earthquake on Jan 09, 2010
Ferndale [b]: Ferndale Earthquake on Feb 04, 2010
Ferndale [c]: Ferndale Earthquake on Feb 26, 2007

Table 2.2: Estimated resonant frequency and average shear wave velocity (*Vs*) for the topmost stratum (Layer 1) in NS direction

Earthquake	Time step (s)	V_s (m/s)	1st resonant frequency (Hz)		Shear Modulus G** (MPa)
			$\frac{V_s}{4H}$	Identified	
Ferndale [a]	0.01	154.5 141.7*	2.27 2.08*	2.13	35.3 29.7*
Weitchpec	0.005	161.9	2.38	2.30	38.8
Bluelake	0.005	161.9	2.38	3.11	38.8
Eureka Offshore	0.01	170.0	2.50	2.62	42.8
Ferndale [c]	0.01	188.9	2.78	2.47	52.8
Ferndale Offshore	0.01	188.9	2.78	2.75	52.8

* during the strong shaking phase 30 s – 35 s.
** using a soil mass density of 1480 kg/m^3

Table 2.3: Estimated resonant frequency and average shear wave velocity (*Vs*) for the topmost stratum (Layer 1) in EW direction

Earthquake	Time step (s)	V_s (m/s)	1st resonant frequency (Hz)		Shear Modulus G (MPa)
			$\frac{V_s}{4H}$	Identified	
Ferndale [a]	0.01	121.4 121.4*	1.79 1.79*	1.90	21.8 21.8*
Weitchpec	0.005	178.9	2.63	2.83	47.4
Bluelake	0.005	154.5	2.27	2.86	35.3
Eureka Offshore	0.01	170.0	2.50	2.65	42.8
Ferndale [c]	0.01	188.9	2.78	3.03	52.8
Ferndale Offshore	0.01	170.0	2.50	2.89	42.8

* during the strong shaking phase 30 s – 35 s.

Figure 2.1: Location of the Eureka Geotechnical Downhole Array (Map data @ 2015 Google) and station photograph (http://www.strongmotioncenter.org)

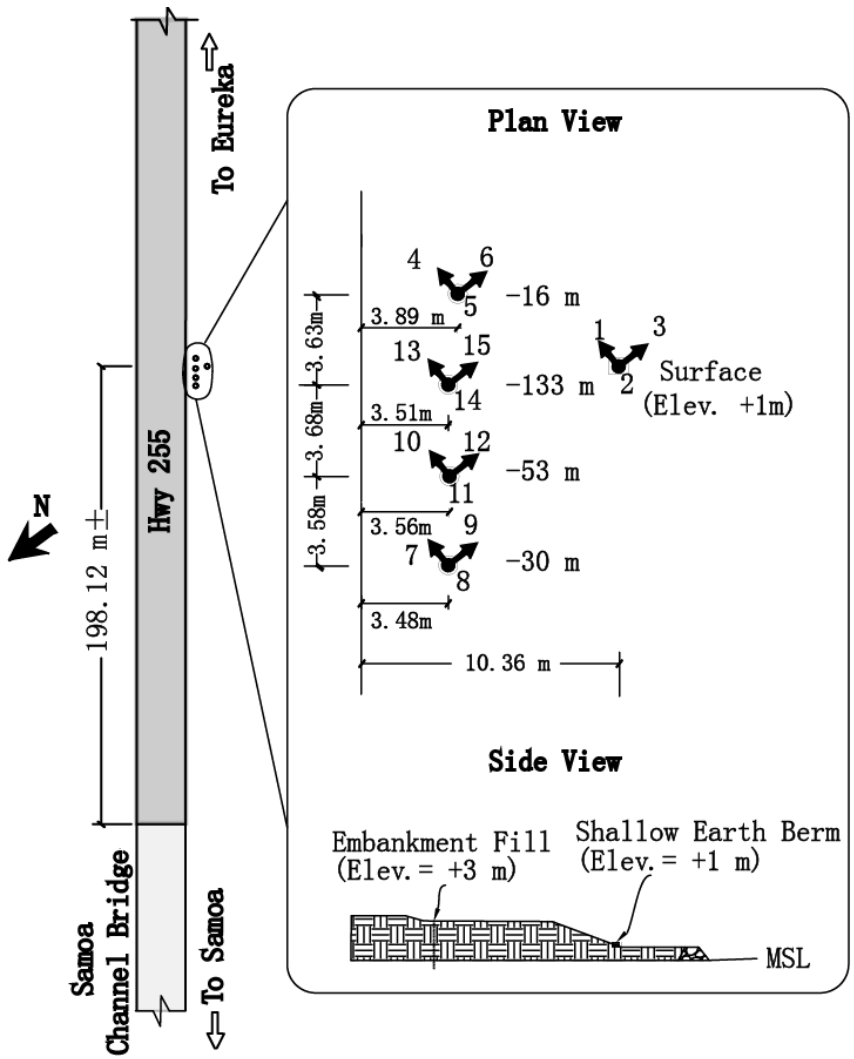

Figure 2.2: The Eureka Geotechnical Downhole Array (http://www.strongmotioncenter.org)

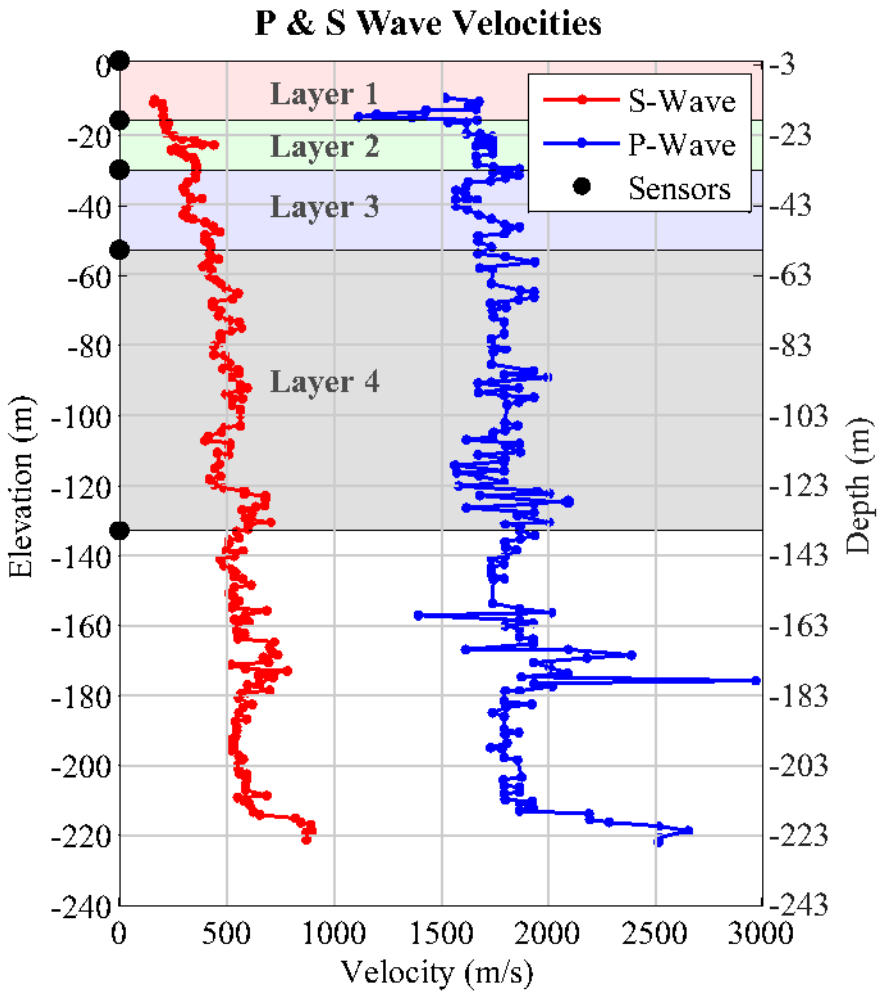

Figure 2.3: Velocity profile along the depth at the Eureka Geotechnical Array (elevation is referenced to MSL) (http://www.strongmotioncenter.org)

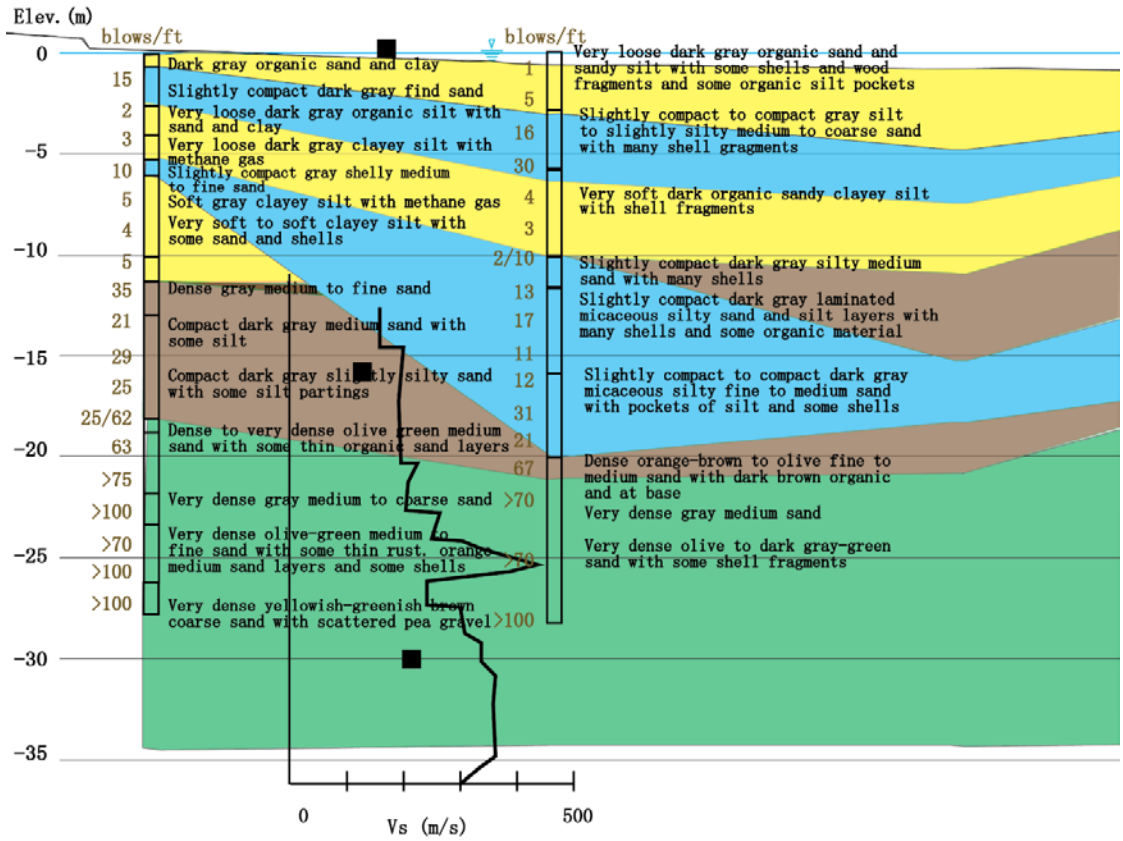

Figure 2.4: Soil profile at the Eureka geotechnical Array site (Caltrans 2002a)

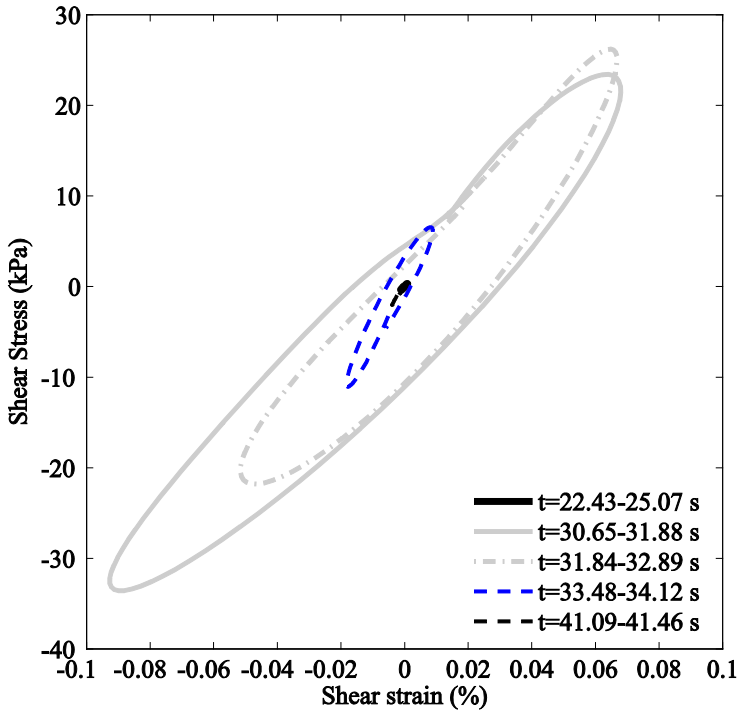

(a)

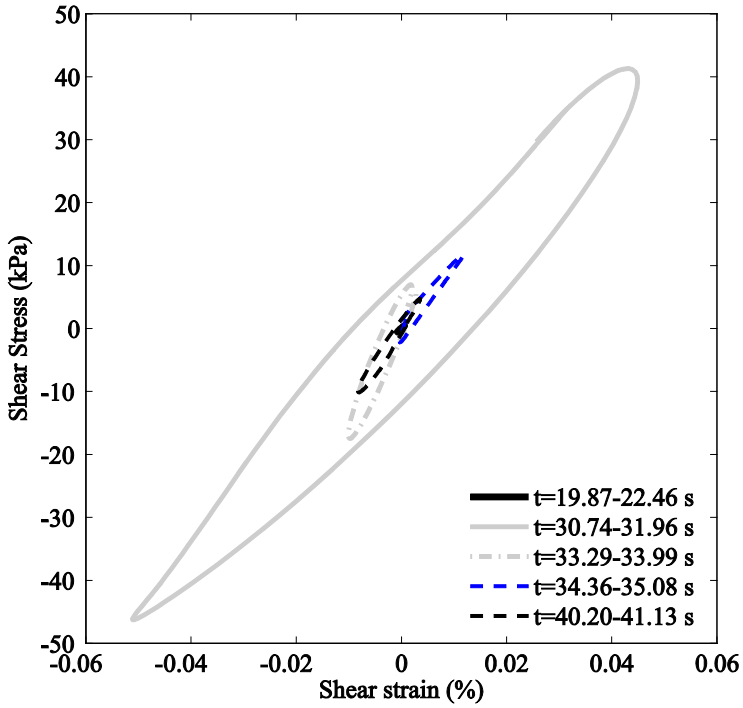

(b)

Figure 2.5: Stress-strain histories for (a) soil layer 1 and (b) soil layer 2 during the moderate event

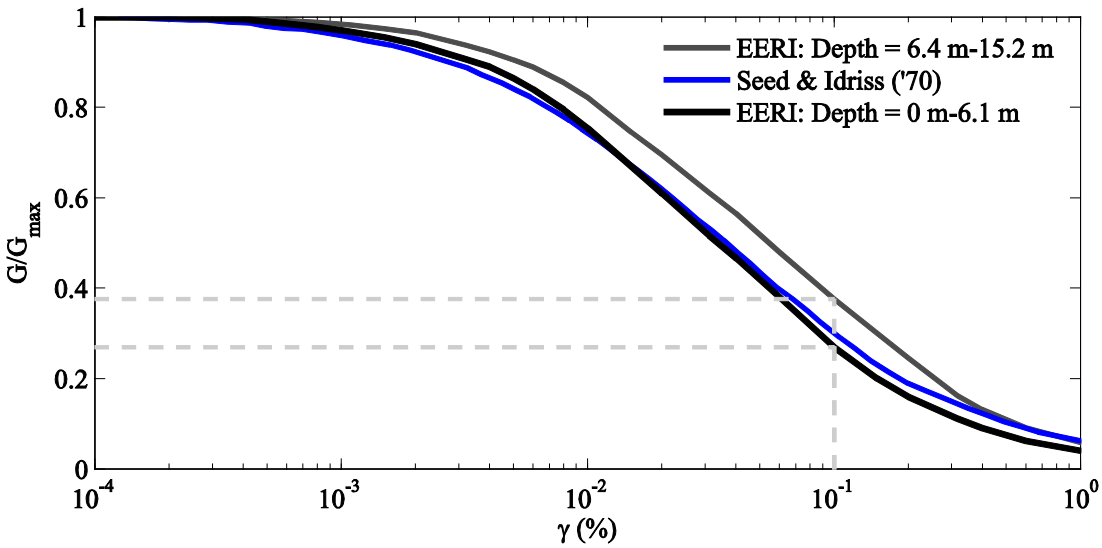

Figure 2.6: Typical range for modulus reduction curves after EPRI (1993) for sand

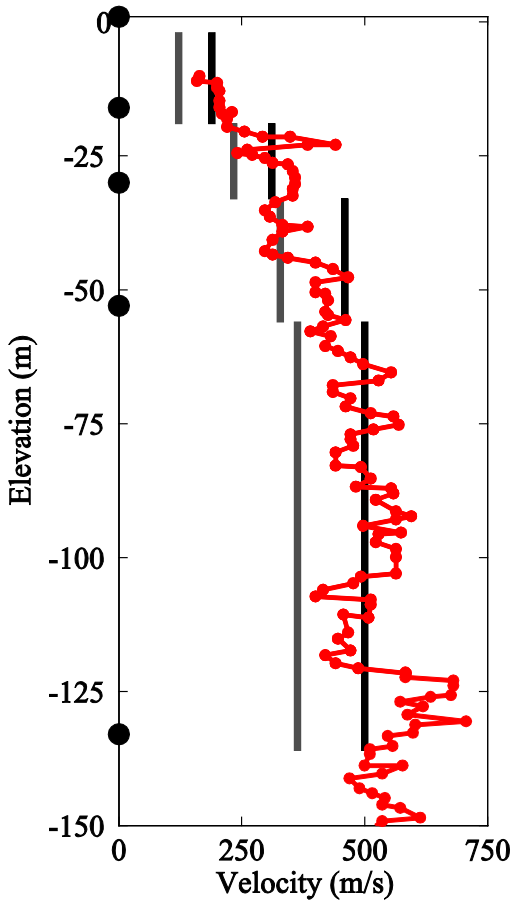

Figure 2.7: Estimates of shear wave velocity in comparison with the geophysical measurements

3 Recorded Seismic Response of the Samoa Channel Bridge System

3.1 Strong-Motion Instrumentations at the Samoa Channel Bridge and Adjacent Downhole Array

3.1.1 General Bridge Information

The Samoa Channel Bridge (SCB) connecting the Samoa Peninsula and Indian Island (Figure 3.1) is one of three bridges crossing Humboldt Bay in Eureka, California. It was designed in 1968, constructed in 1971 and initiated a seismic retrofit in 2002 (Caltrans 1968; Caltrans 2002b).

This 20-span bridge is a 764 m long and 10.4 m wide structure (Figure 3.2). The superstructure consists of cast-in place reinforced concrete deck (16.5 cm of thickness) and four precast, prestressed concrete I-girders. The bridge I-girders are supported on 19 concrete single column type piers and seat-type abutments. The piers and abutments are numbered S-1 through S-21 from the Indian Island side to the Samoa Peninsula side (Figure 3.2). The length of span ranges from 36.576 m to 68.58 m. As shown in Figure 3.2b, there are eight separation joints along the bridge superstructure. Between Pier S-8 and Pier S-9, there is a 50.292 m long prestressed precast concrete drop-in span.

The abutments and piers were founded originally on pile-group foundations consisting of driven pre-cast prestressed concrete piles. Referenced to the mean sea level (MSL), elevation of the mud line varies from -15.8 m below Pier S-8 to +0.9 m at Pier S-20 (Figure 3.2a). Eleven pile groups (from S-3 to S-13) have a pile cap located above the mudline with a maximum value of +16.72 m (elevation of cap base) at Pier S-8 (Figure 3.2b and Figure 3.3).

3.1.2 Original Construction and Seismic Retrofit

The Samoa Channel Bridge was designed in 1968 and the construction was completed in 1971. Minor damage was reported after earthquakes in 1992 and 1994. Some repairs and subsequently an initial seismic retrofit were completed by Caltrans prior to 1997. For instance, the bent caps were reinforced and transversely stressed; pipe extenders and cable assemblies were added to selected bents (Caltrans 2002a).

In order to further strengthen the Eureka bridges, an extensive seismic retrofit program was carried out by Caltrans (Caltrans 2002a) in 2002 (Figure 3.3): (1) strengthening of the foundations by installing additional cast-in-steel shell (CISS) piles (e.g. 6 additional 1.52 m diameter, 19 mm shell thickness piles at Pier S-8), (2) adding or enlarging pile caps to cover the new piles, and (3) encasing the bridge columns in reinforced concrete column jackets. Detailed design drawings, retrofit information along with soil borings are reported by Caltrans (Caltrans 1968; Caltrans 2002b).

3.1.3 Instrumentations of the Samoa Channel Bridge

To obtain insights for both the properties of earthquake and seismic response of the structure, the Samoa Channel Bridge is heavily instrumented with a total of 33 accelerometers (deployed mostly in 1996). Side view and deck level plan view of the sensor network layout for the bridge are shown in Figure 3.2. Locations of sensors are marked with numbered arrows indicating the direction of measured motion.

There are 24 sensors placed on the Samoa Channel Bridge to measure the translational motions of the structure, including 16 on the deck, 3 at the abutments and 5 at the pile caps of Pier S-8 and Pier S-14. Sensors on the structure are oriented in the longitudinal and transverse

direction of the bridge. At a nearby ground surface station (denoted here as BGS, 48.77 m west of the Abutment S-21), three sensors were installed at elevation of +2.5 m approximately, oriented in the north-south (NS), east-west (EW) and vertical directions. In addition, 6 accelerometers were embedded inside one of the retrofitted CISS piles at Pier S-8 (Figure 3.3). As such, foundation seismic response at two different elevations (-10.36 m and -16.46 m) was recorded after the structural retrofit.

Of particular interest in this instrumentation is the dynamic response of the foundation relative to bridge structure at the mid-span of Samoa Channel Bridge (Pier S-8). For this purpose records from sensors 10, 8, 30 and 33 (transverse direction) are studied in details in this report to obtain salient resonant frequencies for both the superstructure and the entire ground-foundation-bridge system.

3.1.4 The Adjacent Eureka Geotechnical Array

As discussed in detail in Section 2, the Eureka Geotechnical Downhole Array (denoted here as GDA, CSMIP Station 89734) is located approximately 198 m south-east of the Samoa Bridge Abutment S-1 (Figure 3.4). A relatively deep soft alluvium geological profile with high water table is noted at this location. The very dense soil layer appears approximately 22 m below the ground surface. Nonlinearity of the site seismic response was evident through analysis of this nearby downhole array data. The recorded data at this site allows for a better understanding of the ground seismic response (details provided in Section 2) in which the Samoa Channel Bridge foundations are embedded.

3.1.5 Recorded Earthquake Motions

The bridge is located in a seismically active area of Northern California. Records from a total of eight earthquakes in the period of March 2000 through March 2014 are currently available with Magnitudes from 4.6 M_w (M_w: regional moment magnitude) to 7.2 M_w (Table 3.1 and Table 3.2).

Notable is the 2010 Ferndale (M_w = 6.5) Earthquake (hereafter, referred to as "the moderate event") which occurred approximately 35 km away from Ferndale, CA. The bridge site at a distance of 53.8 km from the epicenter of this earthquake recorded peak acceleration of 0.15 g at the ground surface and 0.37 g on the bridge deck. During this earthquake, the largest relative movement on the bridge structure was 9.6 cm longitudinally and 7.2 cm transversely referenced to the motion of at -16.46 m within the instrumented pile. This moderate event is the first significant earthquake to occur since the retrofit in 2002 resulting in the largest motion recorded on the bridge. However, no significant damage was reported during this earthquake (Storesund et al. 2010).

3.2 Evaluation of the Earthquake Records

All available records after seismic retrofit (with instrumentation on pile foundation) are employed to evaluate the seismic response of the bridge. In the section below, displacement and acceleration time histories during the Ferndale Earthquake in 2010 (the moderate event) and the Ferndale Earthquake in 2007 (low amplitude shaking event) are selected to demonstrate the significant findings.

3.2.1 Ground Motions at the Bridge and Adjacent Downhole Sites

Some insights may be derived from comparison of the recorded ground motions at the bridge and the downhole array sites (Figure 3.4). Synchronization between the bridge and GDA records was done based on the actual digital time stamp for each site (resulting in a time shift of about 2 seconds during the moderate event). In order to compare with the recorded motions along pier S-8, the ground surface records at the bridge site (BGS) and the GDA records were re-oriented in the bridge transverse (Tran) and longitudinal (Long) directions.

On this basis, Figure 3.5 and Figure 3.6 present the moderate event records of: 1) the bridge ground surface station (BGS), 2) the bridge pile foundation (BPF) near the mudline at the elevation of -16.46 m (after azimuthal orientation error corrections as discussed below in section 3.2.3), and 3) the adjacent geotechnical downhole array (GDA). In general, arrival time of the ground surface seismic waves at the GDA and bridge sites differed by around 0.1 second (as judged by cross-correlation analysis).

Keeping the topography and site stratification in mind (Figure 3.4), response at the pile foundation is seen to more closely align with that of the downhole stations (more so than at ground surface). As such, this location along the pile depth appears to be practically moving along with the ground, indicating a level of relatively firm embedment (fixity) at this depth. Similar conclusions can be deduced based on comparison of records from the other available low amplitude earthquake events (Table 3.1 and Table 3.2).

The pseudo-acceleration response spectra (4 different earthquake events), with 5% damping, for the recorded free field motions of the bridge as well as those of the adjacent downhole arrays are shown in Figure 3.7. There is a noticeable amplification effect for the motion at the downhole ground surface compared to those at depths. In particular, spectral

acceleration of the BPF generally falls between those of the downhole at the ground surface and elevation of -30 m in the short period range. It is noteworthy that the pseudo-acceleration of the BGS station is significantly high for periods less than 0.33 second for all four earthquakes. This observed high energy response at low period might be partially due to the soil characteristics at the site (Figure 3.4) and partially from the impact of being close to the bridge.

3.2.2 Seismic Response along the Bridge Deck

As shown in Figure 3.8 and Figure 3.9, relative displacement time histories (referenced to the motions at the -16.46 BPF station) display in-phase behavior in both directions for the two representative earthquake events. Overall, the bridge is noticeably flexible in the mid-span (Channels 10 and 12). For the moderate event, maximum relative displacement at Pier S-8 is 60% larger in amplitude compared to that at the abutment (Chan 3).

In addition, transverse displacement time histories demonstrate clearly the period of vibration due to the pronounced response of the structure in this direction. The observed resonance (Chan 12) is particularly obvious during the low amplitude shaking events with a period of 1.10 second for the entire vibration phase (Figure 3.8a). During the moderate event, the bridge structure displays a period of 1.57 second during the strong shaking phase of this event (about 28 s – 33 s), which is then reduced to about 1.29 thereafter (Figure 3.9a).

In the longitudinal direction, the displacement (Figure 3.8b and Figure 3.9b) displays a period of 0.75 second for the low amplitude shaking events and 1.27 – 1.50 second for the moderate event. In general, the bridge structure is stiffer in this direction with a lower response period. However, the bridge displays some flexibility during the moderate event, potentially due to partial opening/closing of the separation joints.

3.2.3 Seismic Response of Pier S-8

Given the discontinuity of the bridge structure due to existence of separation joints near Pier S-8, transverse motion of the corresponding central intermediate bent may be analyzed individually in order to glean some initial insights (independent of the rest of the bridge). Additionally, the high transverse motion observed at Pier S-8 (Figure 3.8 and Figure 3.9), indicates the deck support flexibility at this location. As such, of particular interest in this study was the dynamic response of the bridge structure relative to the pile foundation in the transverse direction at mid-span Pier S-8. The observed behavior of this full-scale pile-deck foundation system during actual earthquake events is extremely valuable and will contribute considerably to our current understanding of this important SSI mechanism.

Displacements of the bridge along Pier S-8 (including deck level, pile cap level and the pile below ground) are shown in Figure 3.10 - Figure 3.11. It is observed that the data from the retrofitted pile at elevations of -10.36 m and -16.46 m were out of phase (Figure 3.12). Due to the uncertainty of sensor orientations on the retrofitted pile, cross-correlation analyses were performed. It was found that sensors at the BPF station need to be rotated 103 degrees (counterclockwise) to achieve peak cross-correlation between the BGS motions and the BPF response (in the lateral directions). Meanwhile, about 144 degrees of rotation (counterclockwise) would be needed at the elevation of -10.36 m to correlate the response at -10.36 m to the motions at the pile cap level (Wang 2015). After rotation, motions along Pier S-8 display in-phase behavior in the transverse and longitudinal directions (Figure 3.10 - Figure 3.11). Shamsabadi et al. (2014) obtained similar orientation angles using the Fourier Spectra method.

Transverse displacement records along Pier S-8 at four different elevation are shown in Figure 3.13a with a clear in-phase dominant fundamental response period. With the motion of

BPF as “input”, the pile cap and the bridge deck displacements display significant amplification. As shown in Figure 3.13b, much of the bridge displacements at Pier S-8 are due to deformation occurring at the pile cap level, with the bridge deck motions only slightly different from those of the pile cap. Under the maximum deflection of the substructure (displacement of deck, pile-cap and BPF station, marked as time instant 1 in Figure 3.13b), the bridge pier (between the deck and the pile cap) only contributes about 1.4% of the total deformation. This may be taken as an indication that the pier above the pile cap is quite stiff in comparison to the lateral stiffness afforded by the underlying pile group.

In the longitudinal direction, the displacements are more evenly accounted for by the pile group and the column, potentially due to the reduced column stiffness in this direction (Figure 3.14). In general, foundation flexibility can have a significant influence on the seismic response of Pier S-8 and should be considered in the seismic analysis.

3.2.4 Abutment and Bridge Response along Mud-line

Figure 3.15 and Figure 3.16 compare the acceleration/ displacement time histories of bridge base along the ground surface (including motions at the BGS, the BPF, on the pile cap near ground surface and at the bridge abutments). It was observed that displacement time histories are in the same pattern with larger peak values near abutment S-1. In addition, high frequency components were observed from acceleration time histories (Wang 2015) at BGS and at abutment. In the longitudinal direction, spikes were observed at abutment and on the pile cap of Pier S-14 during the moderate event. All these observations indicate that the motions recorded at nearby ground surface as well as motions on S-14 pier footing: i) are affected by the bridge response, and ii) are influenced by the varying topography and irregular soil profile stratification

under the extended bridge domain. As such, typical modeling procedures using a nearby ground surface response spectrum may not fully reflect the actual input excitation complexities.

3.3 System Identification for the Ground-Foundation-Bridge System

Transfer Function (TF) defined as the ratio of the cross power spectral density (P_{yx} (f) with seismic input signal x and output response y) and the power spectral density (P_{xx} (f)) is employed to assess the system and sub-system resonant frequencies.

In the transverse direction, the fundamental frequency for the Deck-Pier sub-system (deck response referenced to pile cap response) at the Pier S-8 is 1.60 Hz during the moderate event and in range of 1.96 - 2.00 Hz (refer as the first mode frequency of the fixed-base superstructure) for all of the other low amplitude earthquakes. A summary of the TF results for 6 earthquake events employing a Hanning window and 25% -50% overlap to reduce the effects of spectral leakage is presented in Table 3.3. The lower predominant frequency during the moderate event reflects nonlinear behavior in the structure (the Pier Deck sub-system).

The first transverse natural frequency of the foundation-bridge system at Pier S-8 is obtained by relating the response of bridge deck at Pier S-8 to that of the pile at elevation -16.46 m (taken here to be a fixed base as discussed above). Since the nearby bridge ground surface (BGS) is potentially somewhat affected by the bridge structure, transfer function between the bridge deck and the BGS is also evaluated.

The fundamental transverse frequency for the bridge was found to be around 0.97 Hz during all of the low amplitude earthquakes and 0.73 Hz during the moderate event (Table 3.4). The lower predominant frequency during the moderate event reflects nonlinear behavior in the structure as well as in the pile-group response. The identified structure resonant frequency generally agrees with the recently reported ambient vibration testing result (Turek et al. 2014).

3.4 Discussion and Conclusions

Post-earthquake ground/structure response analysis with the aid of system identification methods provides useful information to investigate site and structure dynamic behavior. In this section, unique insights into the salient seismic response characteristics of the Samoa Ground-Foundation-Bridge system were obtained on the basis of strong motion records from the bridge and the adjacent geotechnical downhole array (Caltrans 2013).

Comparisons of the measured time-history indicate that: (1) despite the moderately high levels of shaking, the relative displacement between the top and bottom of the bridge column at Pier S-8 remain relatively small; (2) at Pier S-8, much of the bridge lateral deflections are due to movement of the pile cap. Therefore, foundation flexibility should be considered in the seismic assessment for this bridge structure; and (3) displacement time histories at the BGS station and the BPF station follow similar patterns to those at the downhole array, although BGS motions reveal some additional energy around the high frequency of3.8 Hz . As such, the BPF motion could be a candidate input motion for a computer model of this simplified foundation-structure system.

System identification techniques are applied to the recorded bridge motions to estimate the structure resonant frequencies. The primary findings on the basis of spectral analysis include: (1) Nonlinearity of surrounding soil during the moderate shaking event; (2) Variation of stiffness for bridge column/foundation for different earthquakes and (3) Effects of pile foundation flexibility on the seismic response of the Samoa Channel Bridge.

The results of this research are of significance to the current state of practice in seismic ground-foundation-structure analysis. The performance of bridges during the earthquake events can be explicitly interpreted based on studied full-scale ground/structural response records. In

this domain of highly expensive and time consuming foundation design and retrofit methodology, valuable insights into the ground-foundation-structure seismic response can be obtained with increased availability of strong motion data sets in the future.

Table 3.1: Recorded peak acceleration for recent earthquakes at the Bridge Site (arranged by order of peak acceleration)

Earthquake	Epicentral Distance (km)	Tran. Peak Acc. (g)		Long. Peak Acc. (g)		Vert. Peak Acc. (g)	
		Ground	Structure	Ground	Structure	Ground	Structure
Ferndale* Jan 09, 2010	53.8	0.158	0.665** 0.216***	0.167	2.225** 0.660***	--	1.003
Trinidad June 24, 2007	63.8	0.025	0.063	0.015	0.021	0.008	0.072
Ferndale Mar 09, 2014	81.3	0.019	0.069	0.015	0.033	--	0.064
Trinidad August 16, 2008	40.2	0.016	0.026	0.018	0.043	--	0.056
Willow Creek April 29, 2008	56.6	0.014	0.032	0.010	0.019	--	0.025
Ferndale Feb 26, 2007	62.4	0.011	0.022	0.009	0.016	0.004	0.013
Crescent City June 14, 2005	153.4	0.009	0.031	0.007	0.018	0.004	0.026
Cape Mendocino March 16, 2000	102.4	0.008	0.018	0.004	0.020	0.004	0.009

* the January 2010 Ferndale Earthquake will be referred to as “the moderate event” in this study
** large peak acceleration due to spikes from separation joints
*** estimated after removing spikes using a band pass filter

Table 3.2: Recorded peak displacement for recent earthquakes at the Bridge Site

Earthquake	Epicentral Distance (km)	Tran. Peak Disp. (cm)		Long. Peak Disp. (cm)		Vert. Peak Disp. (cm)	
		Ground	Structure	Ground	Structure	Ground	Structure
Ferndale Jan 09, 2010	53.8	4.519	9.068	6.808	15.927	---	1.847
Trinidad June 24, 2007	63.8	0.152	0.445	0.051	0.124	0.015	0.275
Ferndale Mar 09, 2014	81.3	2.148	3.974	1.370	1.788	---	0.608
Trinidad August 16, 2008	40.2	0.052	0.302	0.084	0.203	---	0.217
Willow Creek April 29, 2008	56.6	0.102	0.652	0.092	0.317	---	0.141
Ferndale Feb 26, 2007	62.4	0.087	0.364	0.156	0.438	0.029	0.060
Crescent City June 14, 2005	153.4	0.128	0.518	0.081	0.275	0.079	0.121
Cape Mendocino March 16, 2000	102.4	0.095	0.604	0.050	0.343	0.035	0.072

Table 3.3: Identified resonant frequency of bridge pier in the transverse direction

Earthquake	Pier S-8 Fundamental Frequency (Hz) $\frac{\text{Deck}}{\text{Pile Cap}}$	
	50% overlapping*	25% overlapping*
Ferndale Jan 09, 10	1.60	1.67
Trinidad June 24, 07	2.00	1.96
Ferndale Mar 09, 14	1.97	1.97
Trinidad Aug 16, 08	1.96	2.00
Willow Creek April 29, 08	1.93	2.00
Ferndale Feb 26, 07	1.93	1.96

* time window is divided into 3 sections but not exceed 30 s

Table 3.4: Identified resonant frequency of bridge system in the transverse direction

Earthquake	Pier S-8 Fundamental Frequency (Hz)	
	$\frac{\text{Deck}}{\text{Pile @} - 16.46\text{ m}}$	$\frac{\text{Deck}}{\text{Free Field}}$
Ferndale Jan 09, 10	0.73	0.73
Trinidad June 24, 07	0.93	0.93
Ferndale Mar 09, 14	0.90	0.87
Trinidad Aug 16, 08	1.00	0.96
Willow Creek April 29, 08	0.97	0.93
Ferndale Feb 26, 07	0.93	0.93

Figure 3.1: Photo of the Samoa Channel Bridge (http://www.strongmotioncenter.org)

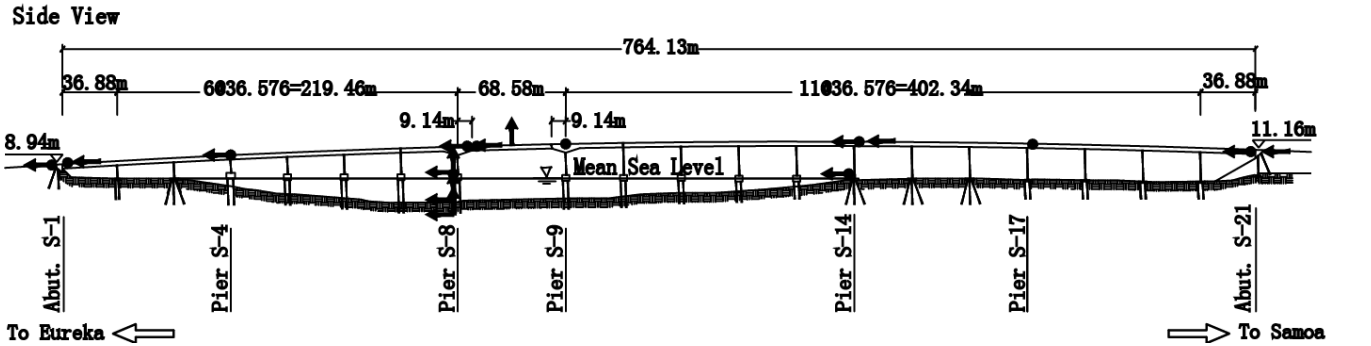

(a)

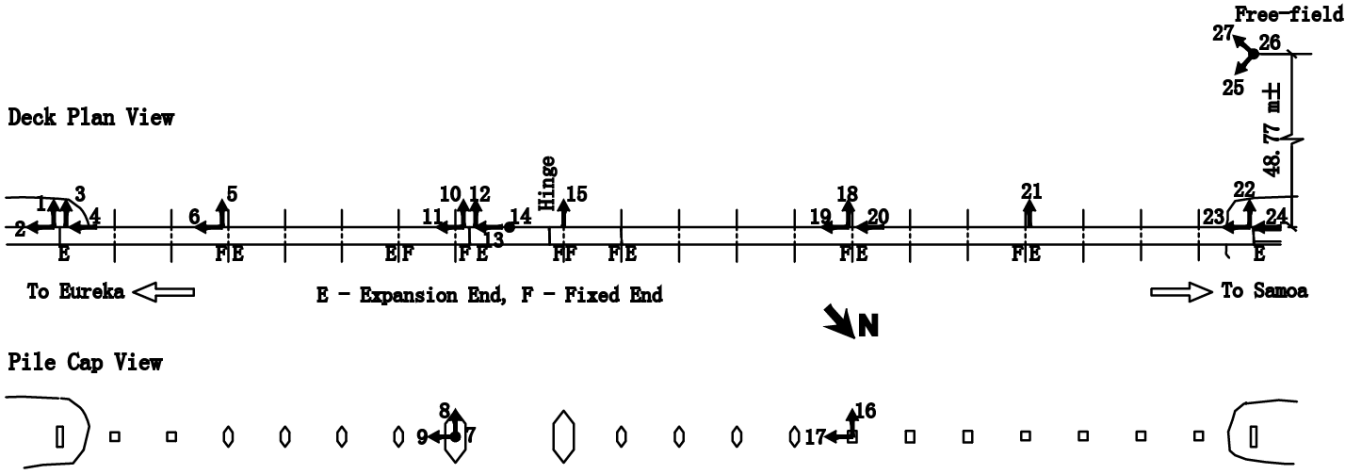

(b)

Figure 3.2: Layout of instrumentation at the Samoa Channel Bridge (http://www.strongmotioncenter.org)

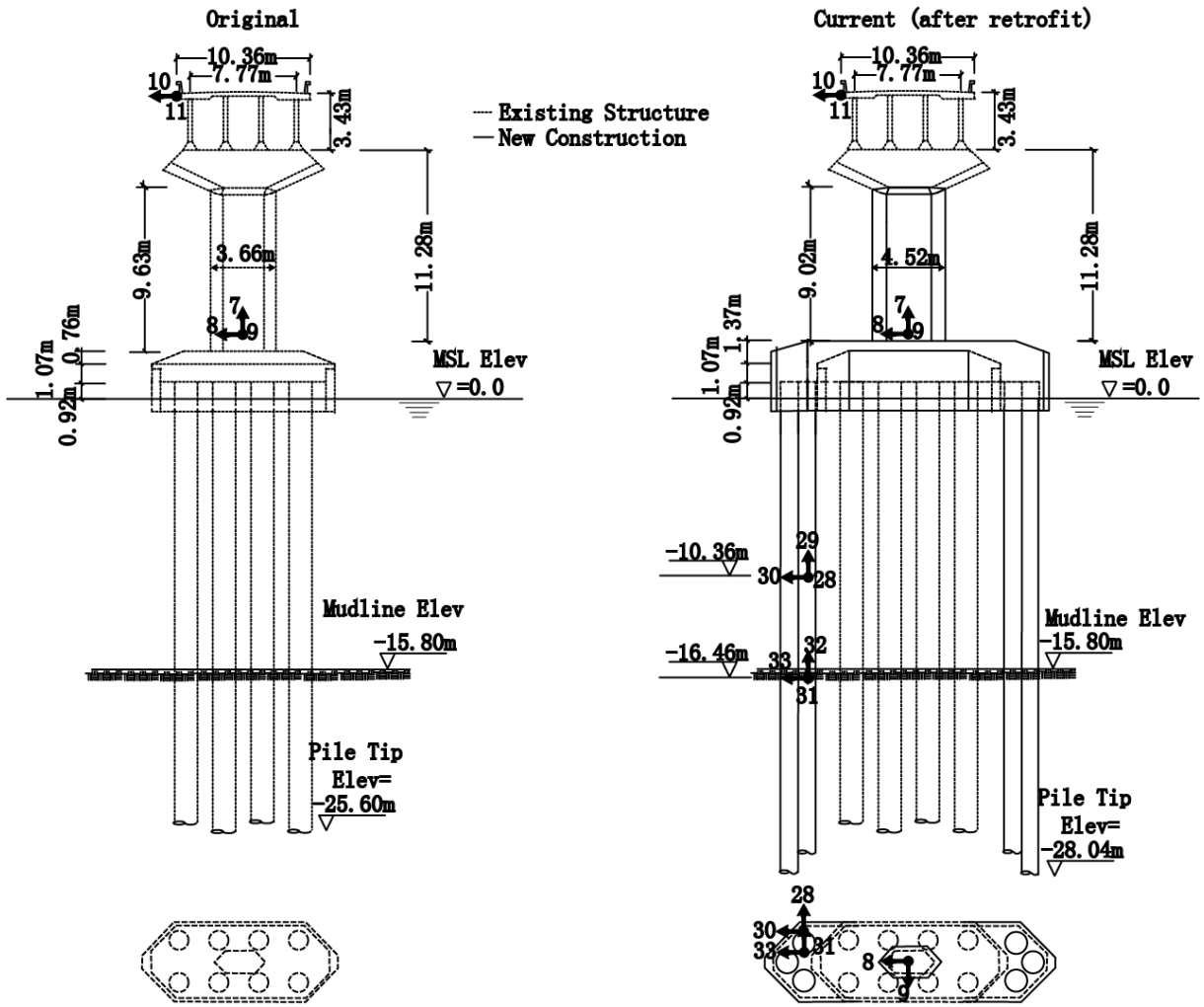

Figure 3.3: Layout of instrumentation at the Samoa Channel Bridge Pier S-8 (Caltrans 2002a)

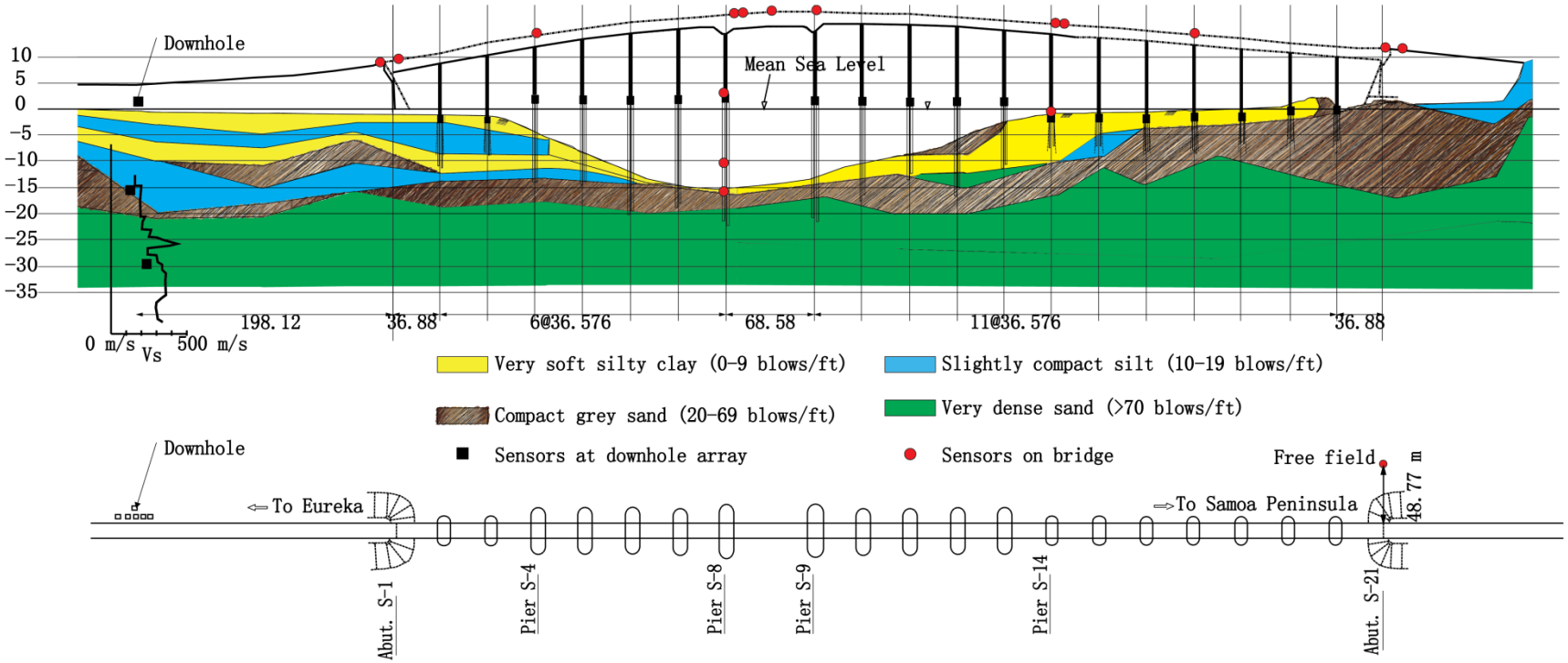

Figure 3.4: Soil Profile along the bridge (Caltrans 2002a) and shear wave velocity profile at Eureka Downhole array (http://www.strongmotioncenter.org)

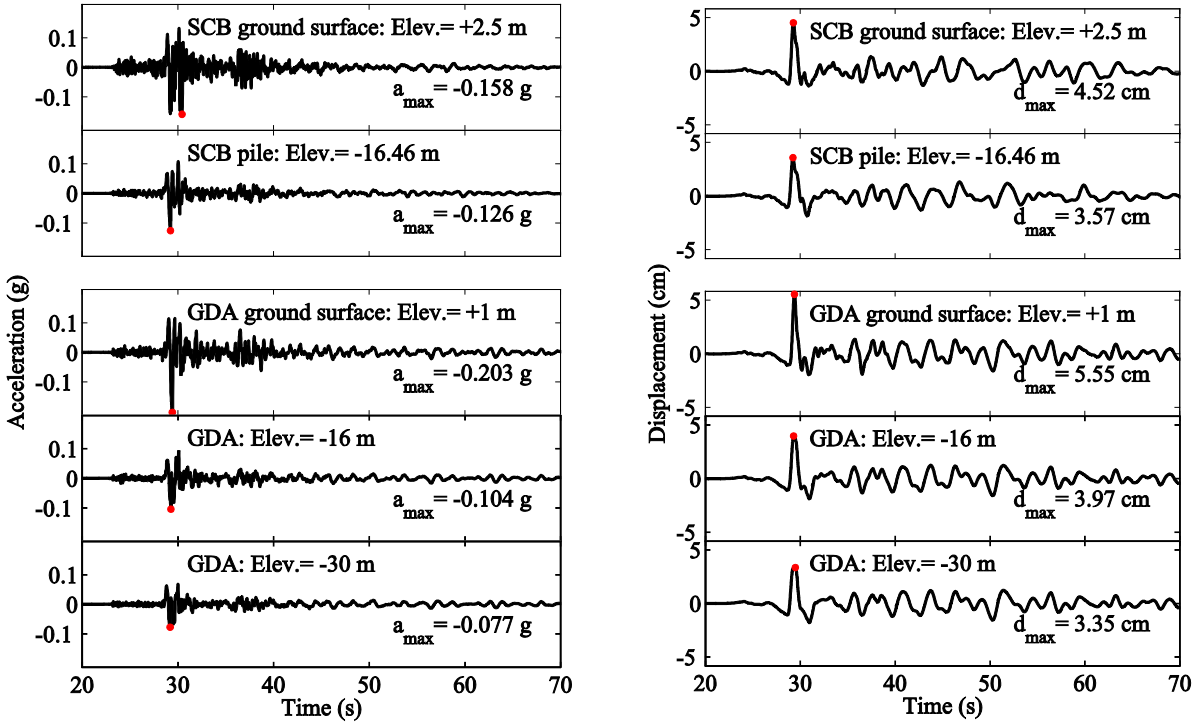

(a) (b)

Figure 3.5: Transversal time histories: (a) acceleration and (b) displacement at the BGS, BPF and GDA stations during the moderate event

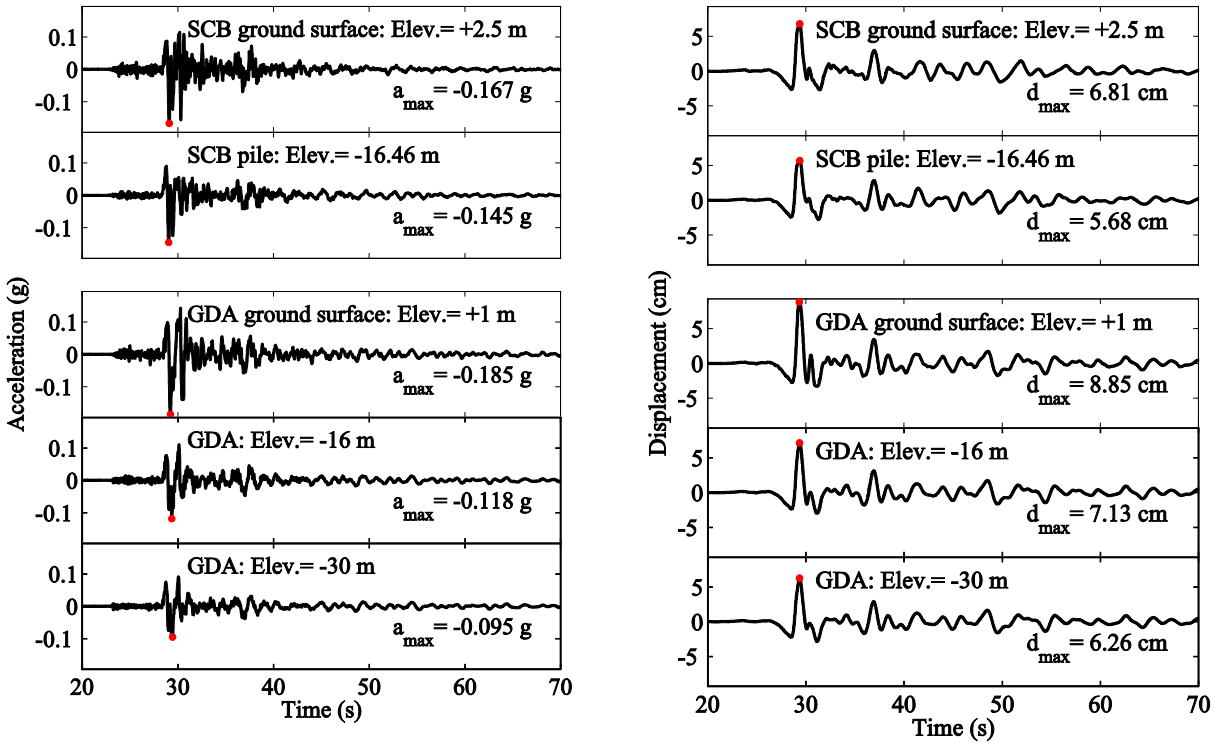

(a) (b)

Figure 3.6: Longitudinal time histories: (a) acceleration and (b) displacement at the BGS, BPF and GDA stations during the moderate event

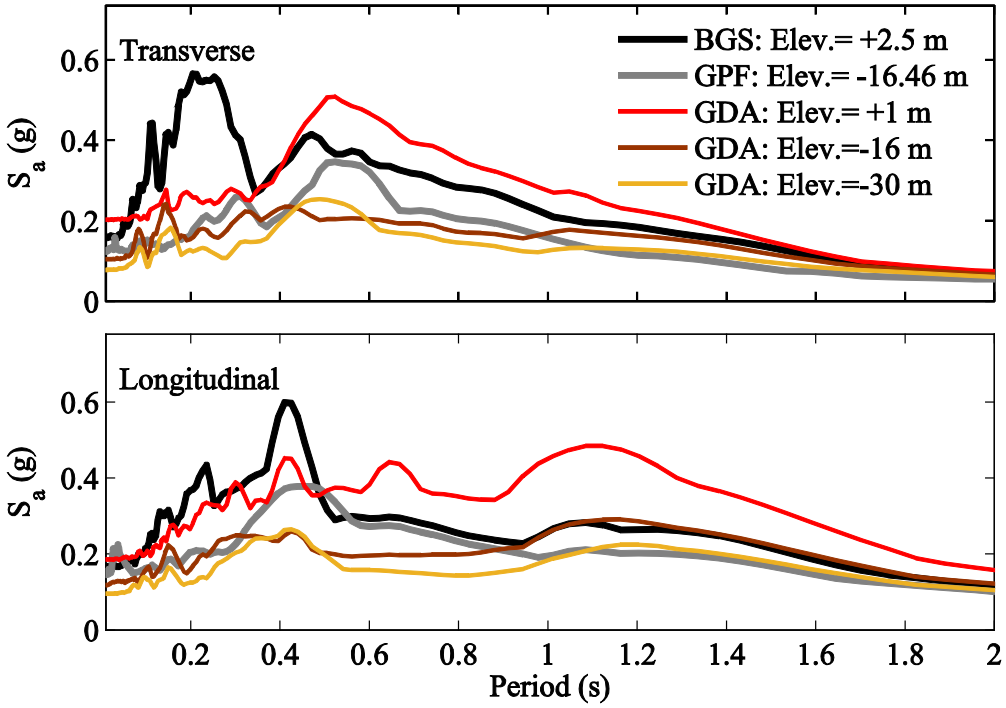

(a)

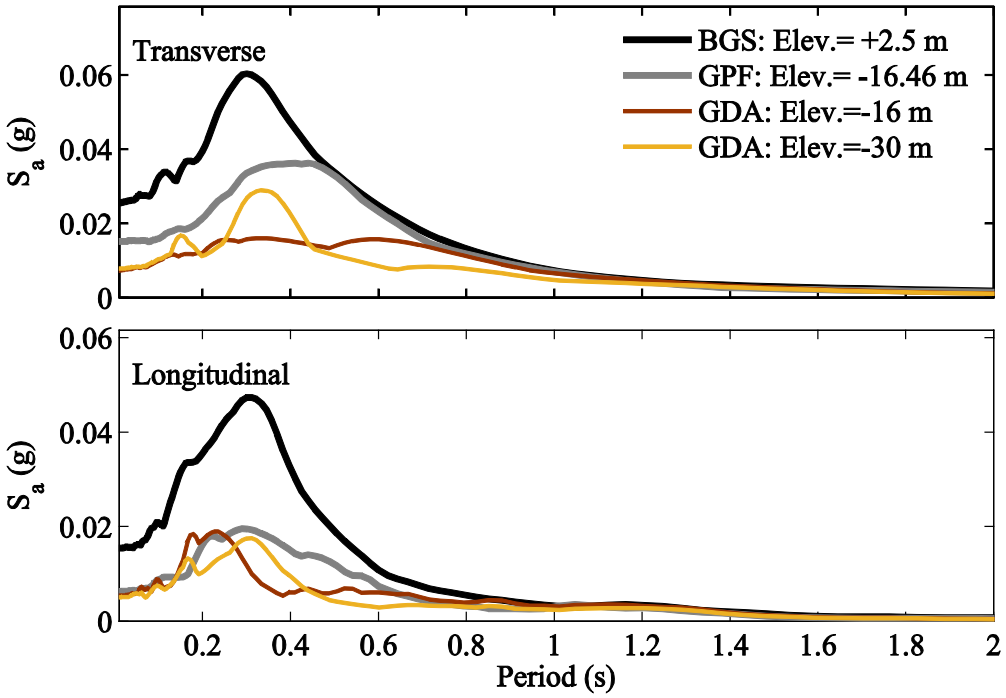

(b)

Figure 3.7: Response Spectra of acceleration of BGS, BPF and GDA at different depths in the transverse and longitudinal directions for: (a) the moderate event and (b) the 2007 Trinidad Earthquake

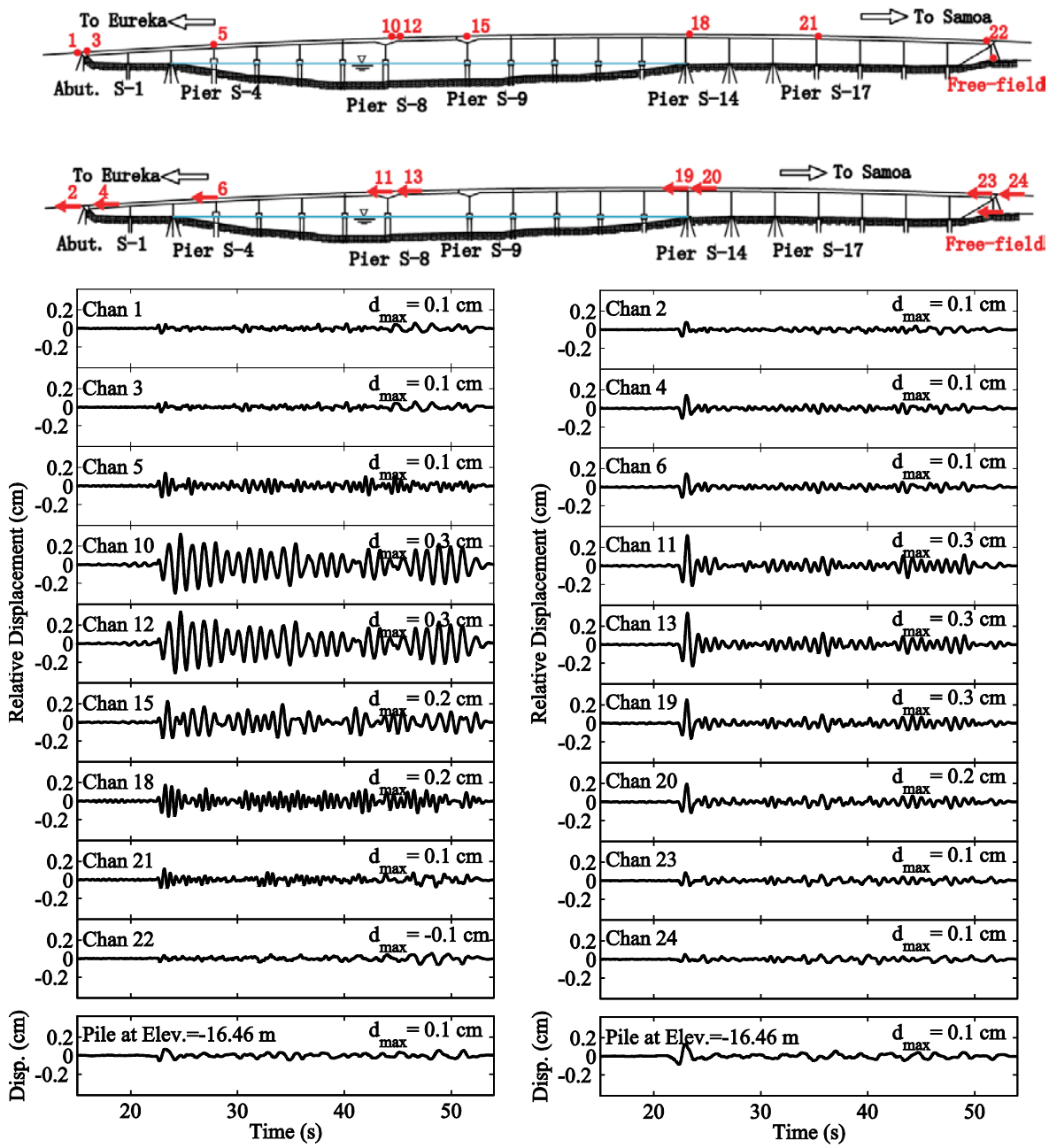

(a) (b)

Figure 3.8: Variation of relative displacement time histories at the bridge deck level for the 2007 Ferndale Earthquake: (a) Transverse and (b) Longitudinal

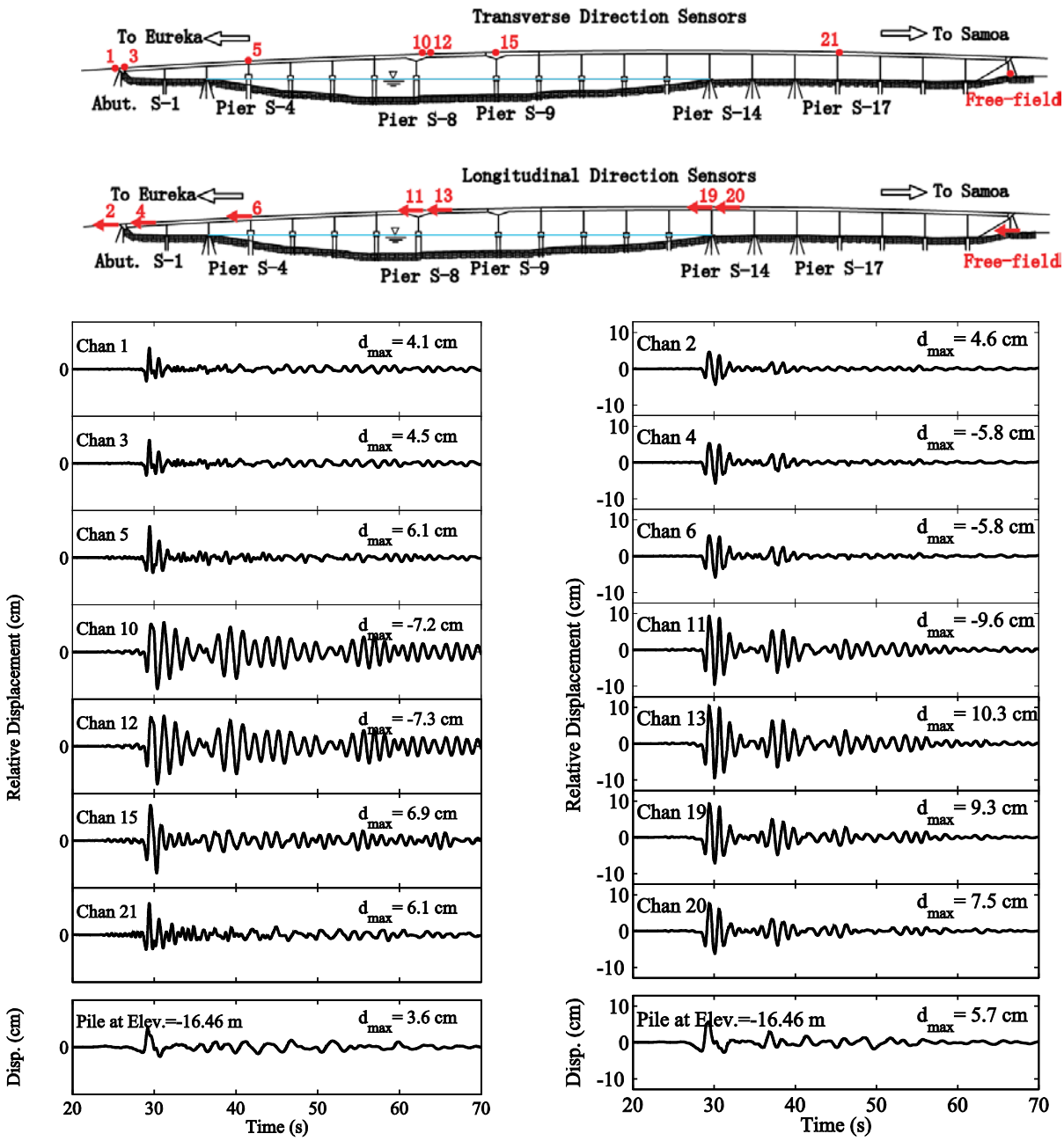

(a) (b)

Figure 3.9: Variation of relative displacement time histories at the bridge deck level for the moderate event: (a) Transverse and (b) Longitudinal

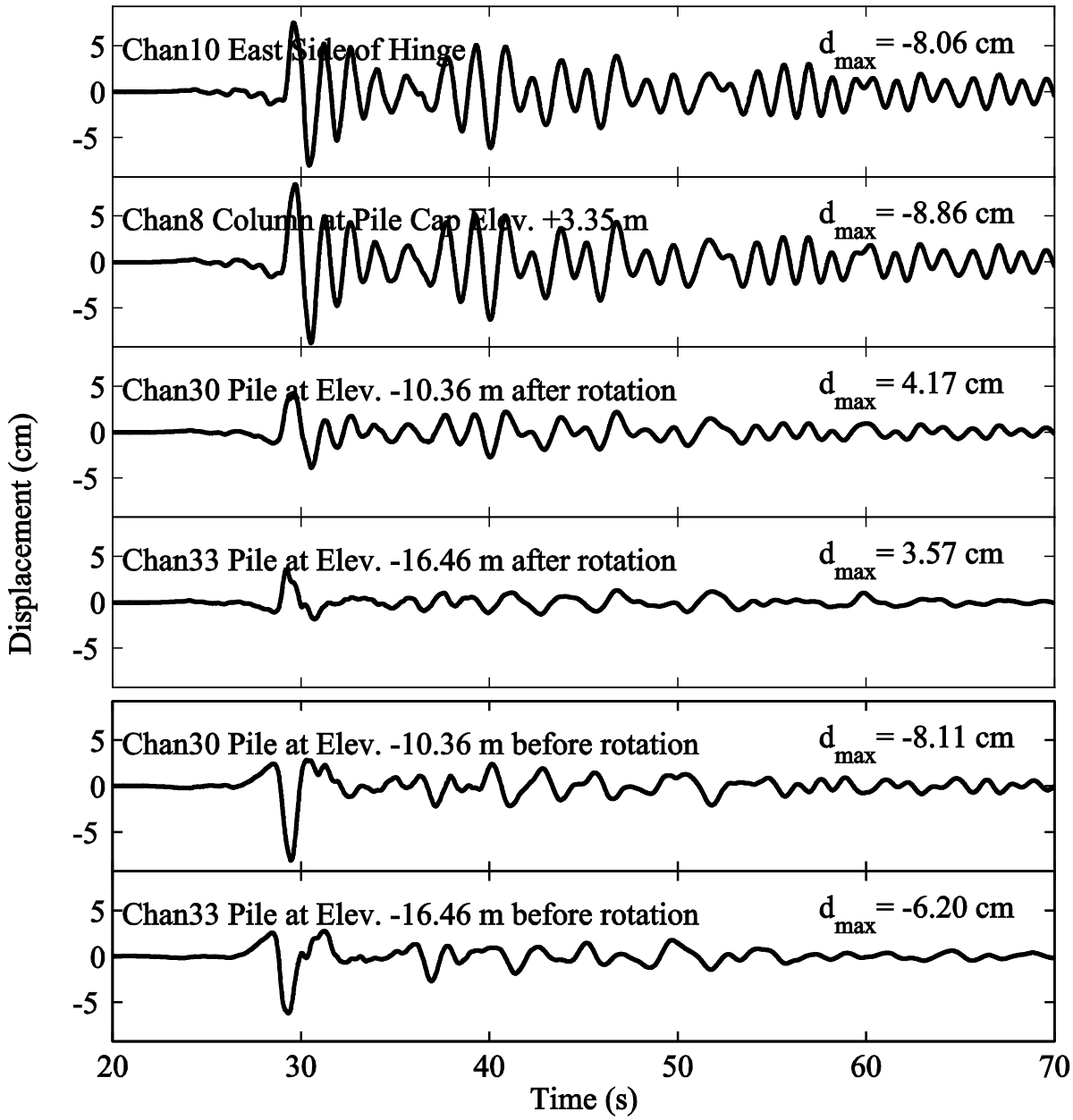

Figure 3.10: Displacement time histories along Pier S-8 during the moderate earthquake in the transverse direction

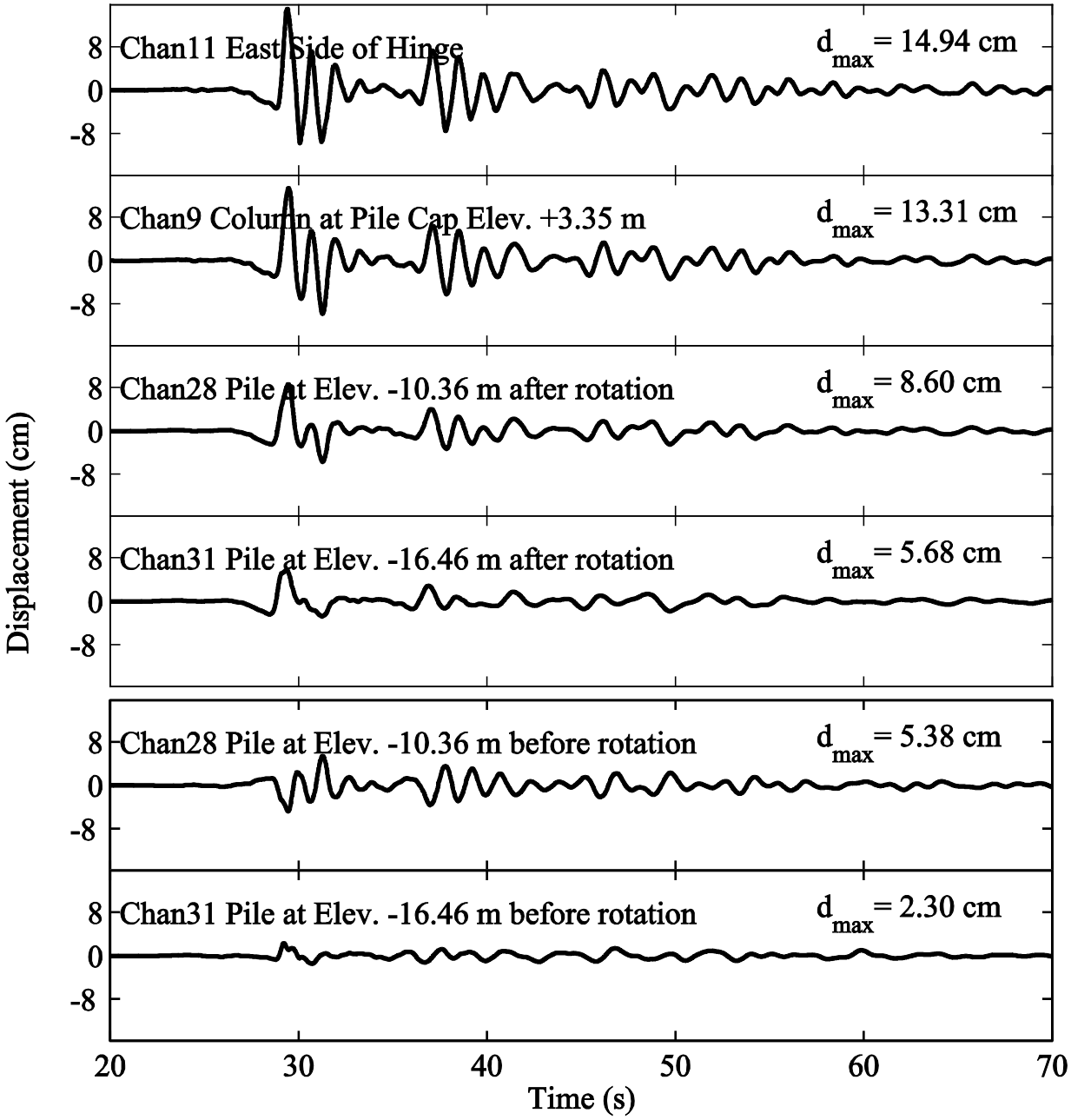

Figure 3.11: Displacement time histories along Pier S-8 during the moderate Earthquake in the longitudinal direction

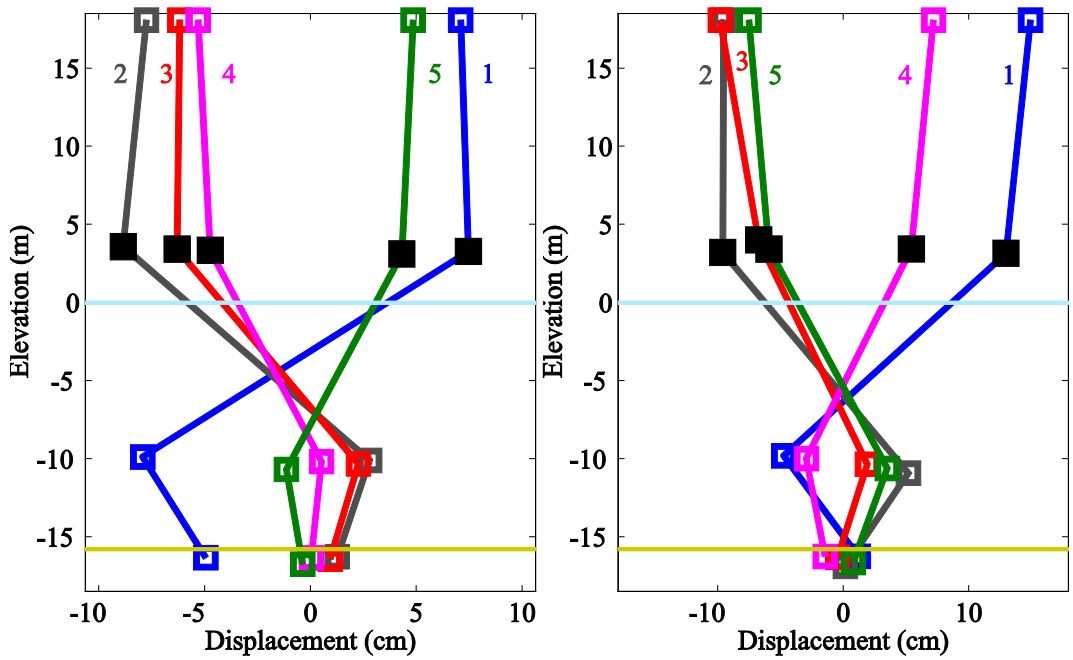

(a) (b)

Figure 3.12: Displaced configuration of Pier S-8 for selected time instants during the moderate event in (a) Transverse and (b) Longitudinal

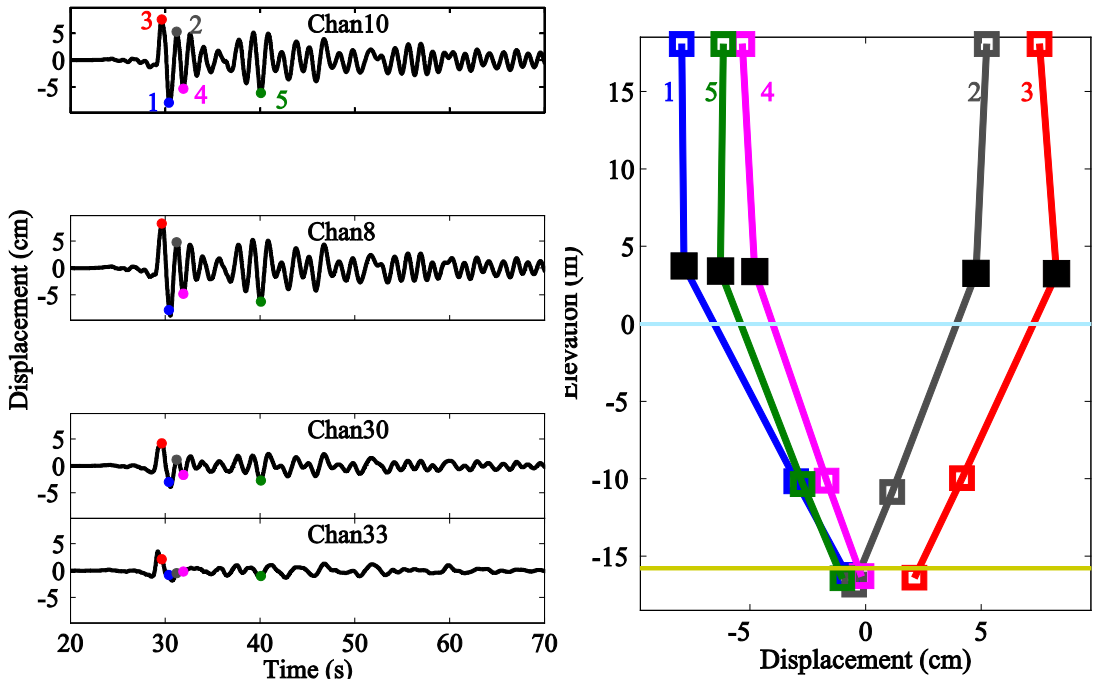

(a) (b)

Figure 3.13: Transverse direction: (a) time histories and (b) displaced configuration of Pier S-8 for selected time instants during the moderate event

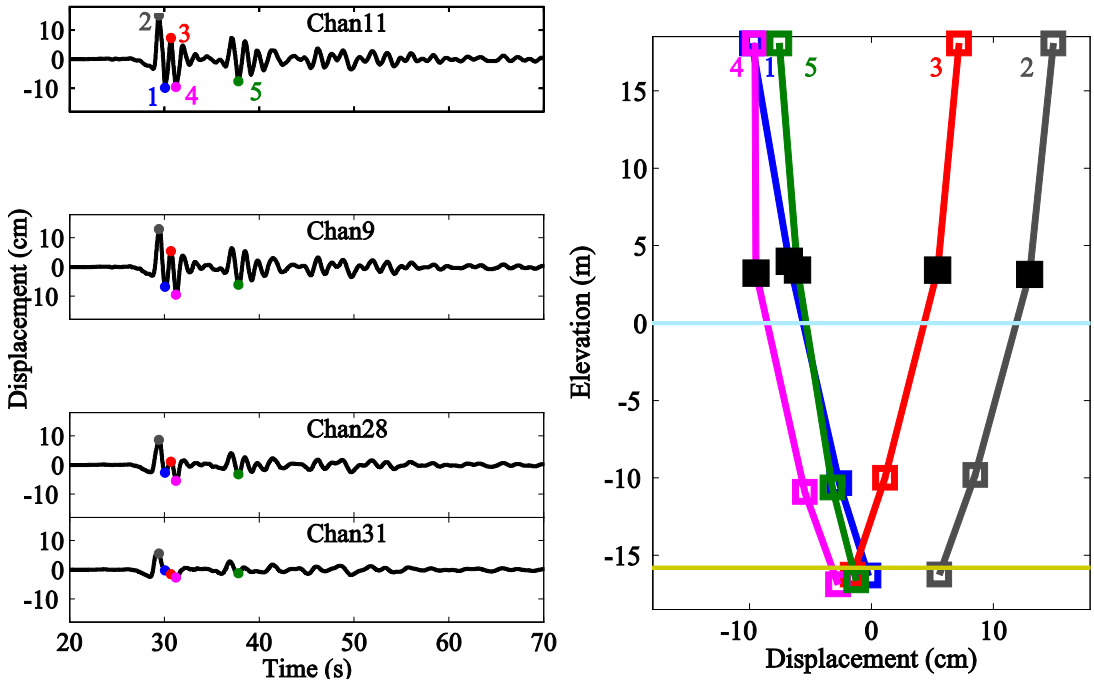

(a) (b)

Figure 3.14: Longitudinal direction: (a) time histories and (b) displaced configuration of Pier S-8 for selected time instants during the moderate event

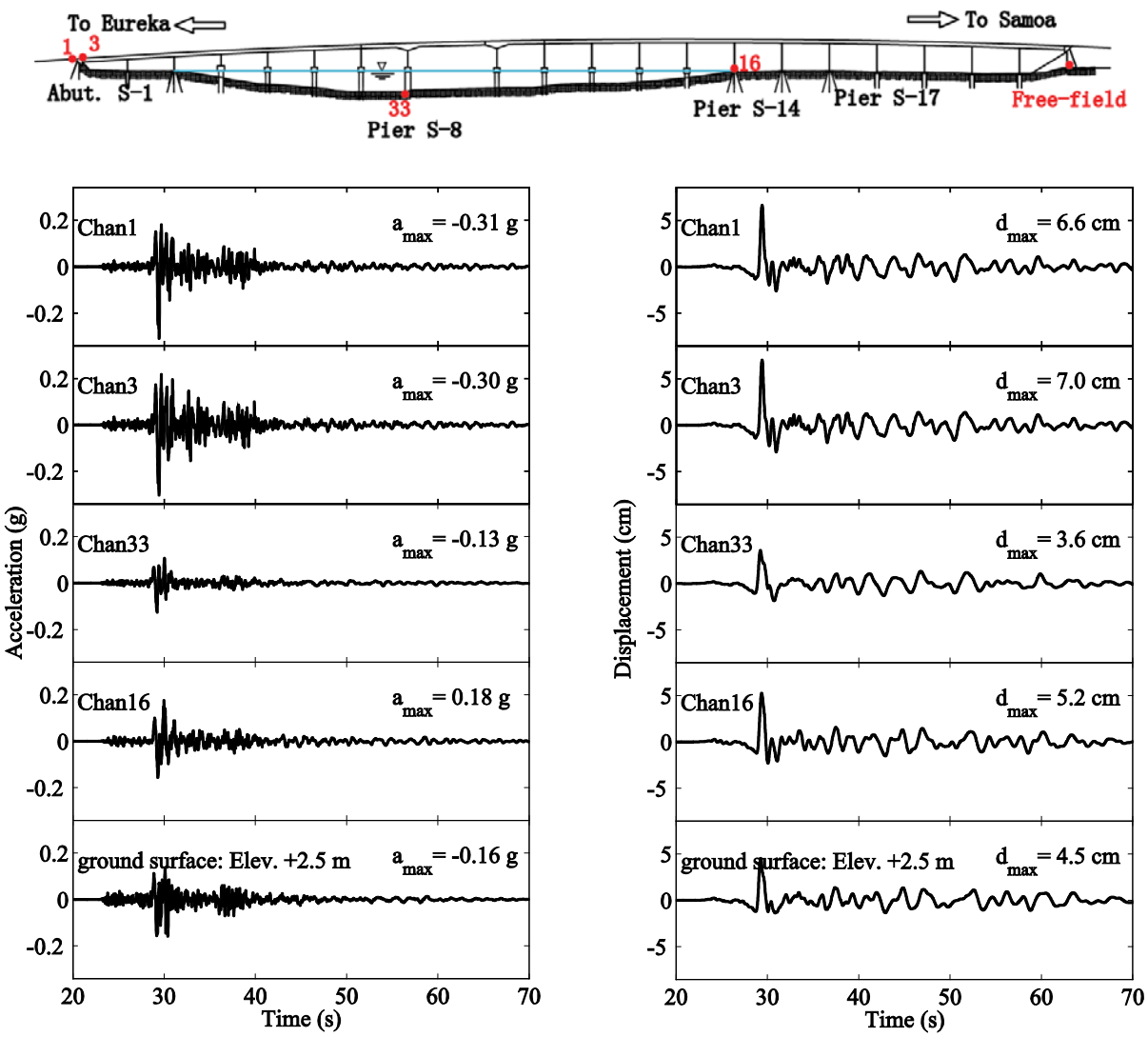

(a) (b)

Figure 3.15: Variation of (a) acceleration and (b) displacement time histories along ground surface in the transverse direction for the moderate event

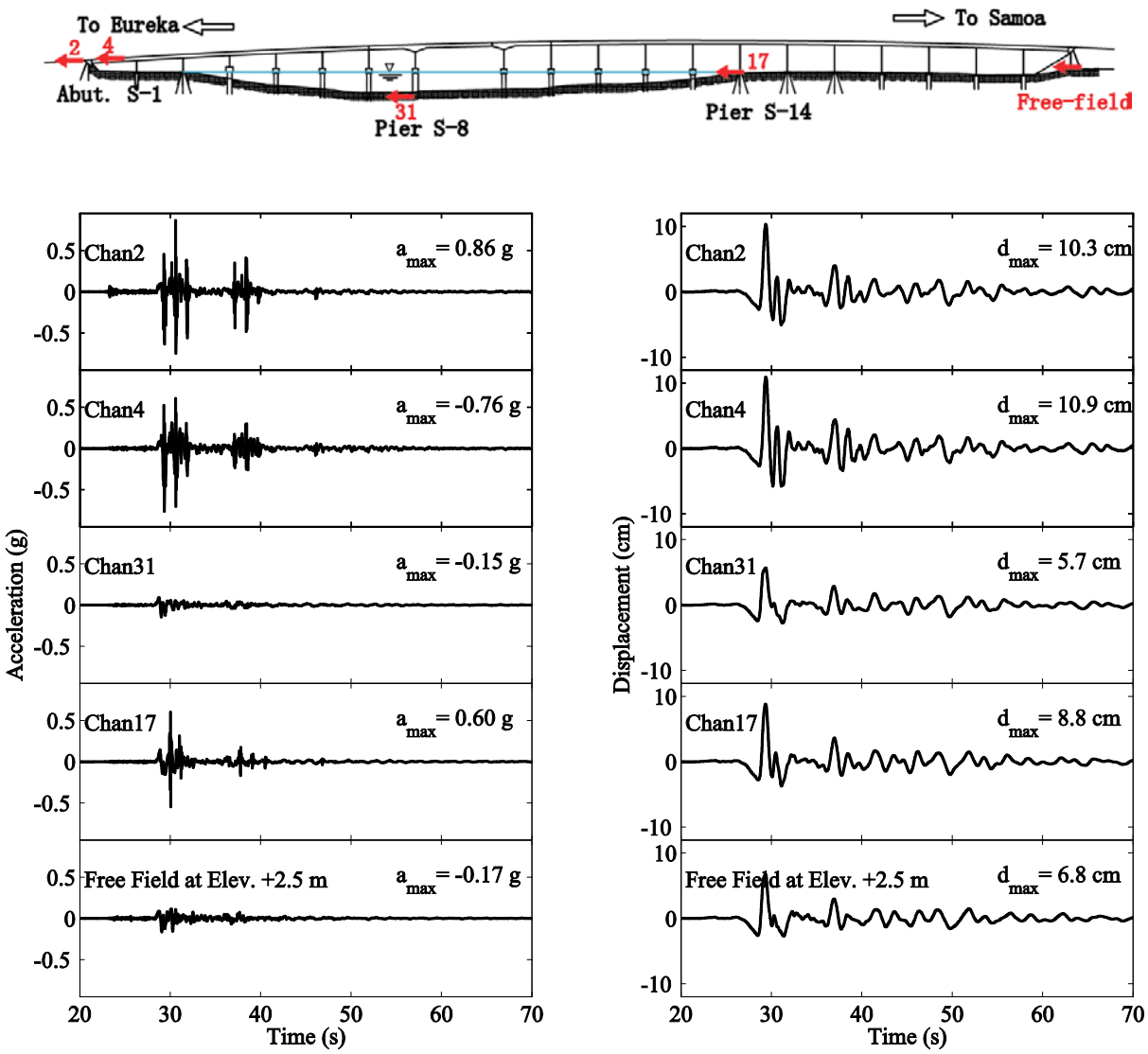

(a) (b)

Figure 3.16: Variation of (a) acceleration and (b) displacement time histories along ground surface in the longitudinal direction for the moderate event

4 Numerical Analysis of the Samoa Channel Bridge System

4.1 Introduction

In section 2.4, extensive seismic records of the Samoa Channel Bridge and the adjacent Eureka Downhole-array are investigated. Resonant frequencies of the foundation-bridge system were identified (Wang and Elgamal 2013). On that basis, the spatial geometry and structural characteristics of the bridge are presented in detail in this section. Linear Finite Element (FE) models of Pier S-8 were developed and calibrated based on the recorded motions and identified bridge/foundation characteristics. Focus is placed on the transverse response of this bent and the estimation of representative stiffness for the bent column and the underlying pile-group foundation. The analyses indicate that during the 2010 Ferndale Earthquake, the estimated lateral stiffness of the pile foundation at Pier S-8 is around 56 percent of that during the other low-amplitude shaking events.

4.2 General Bridge Information

4.2.1 Original Bridge Foundation

Height of the single hexagonal concrete pier columns ranges from 6.19 m at Pier S-3 to 12.9 m at Pier S-14 (Table 4.1). The abutments and pier columns were supported on pile-group foundations. When designed in 1968 (Caltrans 2002a), pile groups under the main span (below Pier S-8 and Pier S-9) consisted of 8 (2x4) prestressed concrete cylinder piles (with diameter D=1.37 m) piles, concrete filled along the entire length, with a 2D center to center spacing. At the reinforced concrete seat type abutments S-1 and S-21, there are 12 square-shaped concrete piles (D=35.6 cm), with 7 battered piles (at a 1:3 ratio) in the front row and 5 vertical piles in the back.

4.2.2 Site Description

Nineteen borings were drilled to a maximum depth of about 34 m below mean sea level (MSL) along HWY 255 in 1968 (Caltrans 1968). Profile Grade of the Samoa Channel Bridge based on the log of test borings (LTB) is shown in Figure 3.4 (Caltrans 2002a). It reveals that the bridge site is mantled by organic fill underlain by dense gray medium to compact gray sand (Caltrans 1968). Very dense coarse gravelly sand was encountered in the bottom layer. Soil layers vary in thickness and are not continuous horizontally. In particular, the surficial foundation soil below Pier S-8 is mainly composed of very soft to soft organic silt with clay (0.9 m). Soil layers consisting of dense to very dense gray medium and sand underlie the surficial soil layer and continue to the maximum explored depth.

4.3 Insights from the FE Analysis of Pier S-8

4.3.1 Finite Element Modeling

In an effort to gain preliminary insights, transverse motion of the intermediate Pier S-8 was studied, independently of the rest of the bridge, based on recorded seismic data (Wang and Elgamal 2013). This idealization is partially substantiated by the extended length of the bridge (764.1 m) and presence of separation joints at adjacent bents, as well as the observed relatively high transverse response flexibility at this near-mid-span location.

As mentioned earlier, the pile cap at this location was observed to undergo significant lateral displacement during the moderate event. As such, one of the key aspects to investigate is the lateral stiffness of the pile foundation. Utilizing the earthquake records in conjunction with model-based system identification techniques, the dynamic transverse response is investigated in view of stiffness for the column and the foundation at this location.

Based on the “as-built” geometry of the bridge, two linear elastic FE models of Pier S-8 (Figure 4.1) are developed using the FE framework OpenSees. These models consist of lumped masses at (1) the center of gravity for the deck I-girders, (2) the pier top, and (3) the pile cap level, connected by bending beams. The masses define center-to-center mass of the superstructure above S-8 (including bridge deck, longitudinal and transversal girders, and hammerhead beam of pier), mass of pier column, pile cap, and pile foundation. Calculations of mass are based on the density and volume of structural components.

The 1st FE model (FEM1 in Figure 4.1) represents the pier column at S-8. The boundary condition at the base of the pier column is considered to be fixed in all DOFs with prescribed input motion (recorded pile cap motion at Chan 8). Possible rotation at the pile cap level was assumed to be negligible due to the underlying spatially large pile group configuration.

The 2nd FE model (FEM2 in Figure 4.1) includes the pier column and the pile group below. Since it has been shown that seismic motion of the retrofitted pile at the elevation of -16.46 m has the same pattern as the motions of the nearby geotechnical downhole array, it was taken as the input excitation for this model. Therefore, boundary condition for the 2nd FE model (FEM2) is considered to be fixed in all DOFs with prescribed transverse motion defined by the record of Chan 33 at the -16.46 m location. In addition, pile cap mass location is assumed to be fixed against rotation (translation allowed only in view of the underlying spatially large pile group configuration). Relatively high bending stiffness (EI) of the pile cap beam-column element is defined to achieve rigidity (this additional element represents the pile cap height).

Material parameters for the simplified FE models were defined based on the as-built drawings as (Caltrans 2002a): reinforced concrete (RC) mass density ρ= 2560 kg/m3, Young’s modulus E=2.79x10^7 kPa (compressive strength $f_c' = 34$ MPa) for the original-construction RC

and Young's modulus E=2.53x10^7 kPa (compressive strength $f_c' = 28$ MPa) for the RC used for retrofit, Poisson's ratio ν=0.2 for concrete, and Steel Young's modulus Es=2.0x10^8 kPa.

4.3.2 Calibration of the Pier Column Model at Pier S-8

Eigenvalue analyses were performed (FEM1) to calibrate the stiffness of pier column (Table 4.2) by matching the fundamental frequency of the FE model with the identified values in Section 3.3. The pier column stiffness defined in this fashion includes contributions from interaction (resistance) due to the overall bridge connectivity. The identified flexural stiffness (EI) of the pier column is contrasted with estimates based on the uncracked section estimates (Table 4.2). The employed quantities amounted to a factor varying from 0.46 (the moderate event) to 0.65 (low amplitude earthquake events). The reduced pier column stiffness agrees with the estimation from moment-curvature analysis of the fiber-section with nonlinear materials under the gravity load (Wang 2015). In addition, these factors are in a range of cracked properties of common Caltrans practice where effective section properties are employed for concrete pier columns (Caltrans 2012; Caltrans 2013).

4.3.3 Calibration of the Pile Foundation Model at Pier S-8

For the FEM2, the pile foundation is taken as a single equivalent super-pile with the union of the cross section of all the piles (Shantz 2013), assuming linear elastic pile behavior. Large EI is set for the pile cap bending stiffness to achieve rigidity. As such, the defined pile foundation flexibility implicitly accounts for SSI.

With identified column stiffness from FEM1, one might calibrate the pile group foundation lateral stiffness to match with the identified bridge resonant frequencies. It turns out that the pile group foundation stiffness (Table 4.3) appears to be noticeably lower than

calculations might imply (only 25% of the estimated EI is engaged) for the moderate event. For the low amplitude shaking events, where the corresponding identified pier stiffness is 0.65 of the uncracked section, the identified pile foundation stiffness reached a higher factor of 0.41 (Table 4.3). Good agreements between the computational results and the actual measurement (Figure 4.2 and Figure 4.3) for both FE models are achieved (Wang 2015). Lower stiffness factors during the moderate event highlight the nonlinear response of the structure.

On this basis, the lateral foundation spring value for the isolated Pier S-8 is evaluated using the available measurements at deck level, pile cap level and in retrofitted pile. The identified spring value (below Pier S-8) is listed in Table 4.6 for six earthquakes. Comparisons between the recorded and the computed time histories are shown in Figure 4.5 for the moderate event. It was found that spring value below S-8 is as high as 8.50×10^4 kN/m during the low amplitude earthquake event and as low as 4.33×10^4 kN/m during the moderate event.

4.4 Conclusions

In this section, salient effects of the ground-foundation system on bridge response are assessed with the help of recorded strong motion data and identification techniques. In particular, bridge pier and foundation lateral stiffness coefficients are estimated.

The results of this research are of significance to the current state of practice in seismic pile-ground-structure analysis. While the identified stiffness estimates might remain subject to further improvements, reference to values derived analytically or by other techniques might prove to be quite beneficial.

Table 4.1: Diameter and height of pier and pile foundation

Pier Number	Pier Height (m)	Existing Piles		Retrofitted Cast-In-Steel Shell Pile*		
		Configuration	D (m)	D (m)	Pile Length (m)	Pile Above Mudline (m)
S-2	7.37	4×4	0.36	0.914[b]	14.63	-2.45
S-3	6.19	4×4[d]	0.36	0.914[b]	16.31	7.32
S-4	7.13	5	1.37[a]	1.524[c]	22.86	7.62
S-5	8.46	5	1.37[a]	1.524[c]	26.22	10.52
S-6	9.58	5	1.37[a]	1.524[c]	28.65	14.32
S-7	10.29	2×3	1.37[a]	1.524[c]	28.04	16.52
S-8	9.02	2×4	1.37[a]	1.524[c]	28.96	16.72
S-9	9.55	2×4	1.37[a]	1.524[c]	26.22	15.22
S-10	11.43	2×3	1.37[a]	1.524[c]	25.30	12.42
S-11	11.10	2×3	1.37[a]	1.524[c]	23.78	9.82
S-12	10.52	2×3	1.37[a]	1.524[c]	22.56	8.02
S-13	10.01	5	1.37[a]	1.524[c]	18.60	4.22
S-14	12.93	4×5 [d]	0.36	0.914[b]	13.72	-2.14
S-15	12.09	4×5 [d]	0.36	0.914[b]	13.72	-2.14
S-16	11.15	4×4 [d]	0.36	0.914[b]	12.19	-2.44
S-17	10.52	4×4	0.36	0.914[b]	11.74	-2.29
S-18	9.81	4×4	0.36	0.914[b]	12.35	-2.29
S-19	8.33	4×4	0.36	0.914[b]	12.19	-1.83
S-20	7.67	4×4	0.36	0.914[b]	12.19	-2.43

* See Wang (2015) for geometric pile group configurations
[a] Prestressed concrete cylinder pile with wall thickness h=0.127 m
[b] Four new Cast-In-Steel Shell Pile with wall thickness h=0.013 m
[c] Cast-In-Steel Shell Pile with wall thickness h=0.019 m
[d] 1:3 Batter

Table 4.2: Uncracked section properties for pier column S-8 (Caltrans 2002a)

Uncracked Section	Pier S-8
Area of Cross Section (m^2)	7.01
Transverse Moment of Inertia (m^4)	7.06
Longitudinal Moment of Inertia (m^4)	1.88
Torsion Constant (m^4)	5.77

Table 4.3: Identified stiffness factor for pier and pile foundation at Pier S-8

Earthquake Event	Stiffness factor based on EI of uncracked section	
	Pier ($EI=1.79\times10^8$ kN-m^2)	Pile Foundation ($EI=8.95\times10^7$ kN-m^2)
Ferndale 01/09/2010	0.46	0.25
Trinidad 06/24 /2007	0.65	0.42
Ferndale 03/09/2014	0.65	0.41
Trinidad 08/16/2008	0.65	0.44
Ferndale 02/26/2007	0.63	0.44
Willow Creek 04/29/2008	0.65	0.41

Table 4.4: Identified frequency and spring value representing pile foundation below Pier S-8

Earthquake	Computed Frequency (Hz)	Identified spring value K (kN/m)
Ferndale 01/09/2010	0.73	4.33×10^4
Trinidad 06/24 /2007	0.93	7.20×10^4
Ferndale 03/09/2014	0.90	6.60×10^4
Ferndale 02/26/2007	0.93	7.20×10^4
Trinidad 08/16/2008	1.00	8.50×10^4
Willow Creek 04/29/2008	0.97	7.90×10^4

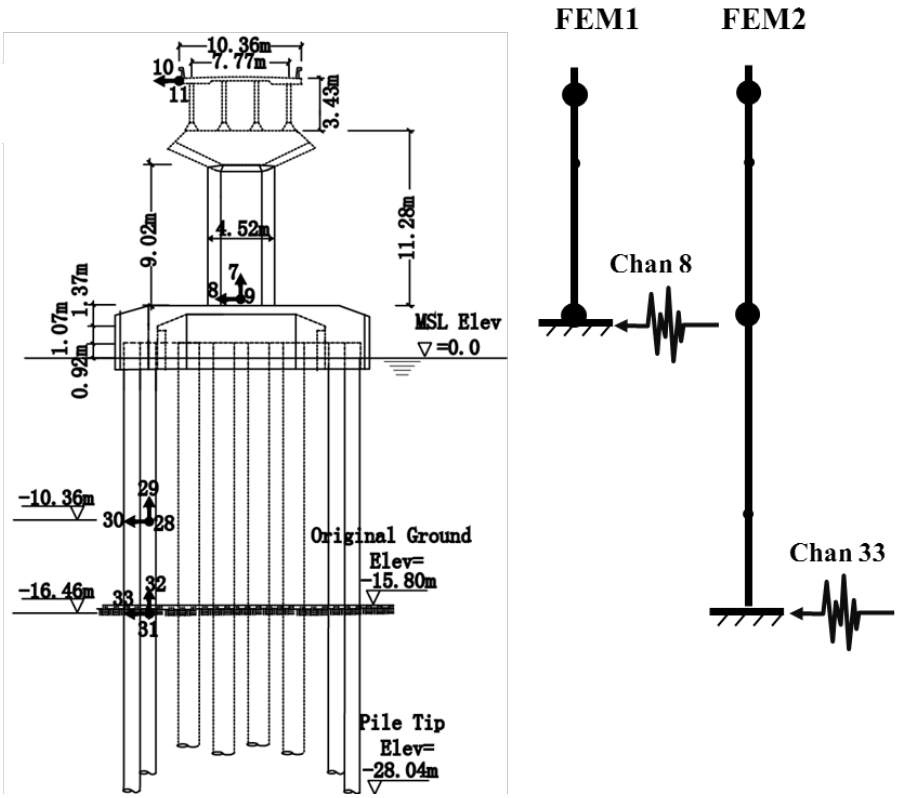

Figure 4.1: Pier S-8 single column type pier model

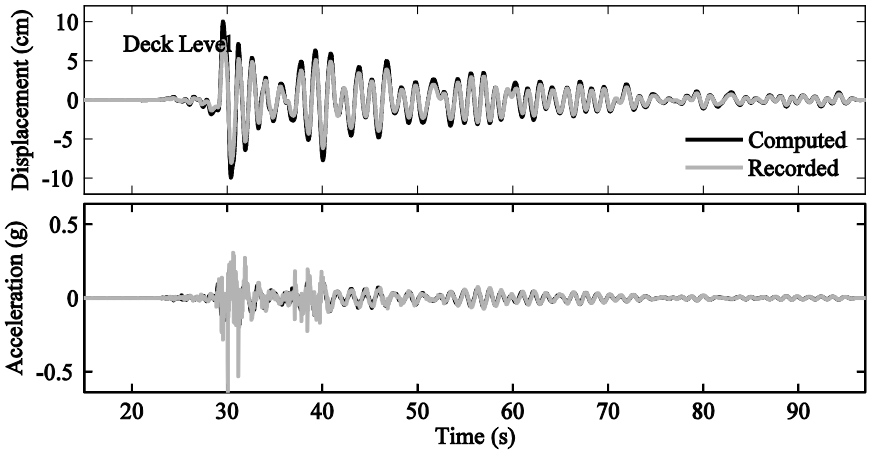

Figure 4.2: Time histories comparisons for at Pier S-8 (deck level) during the moderate event

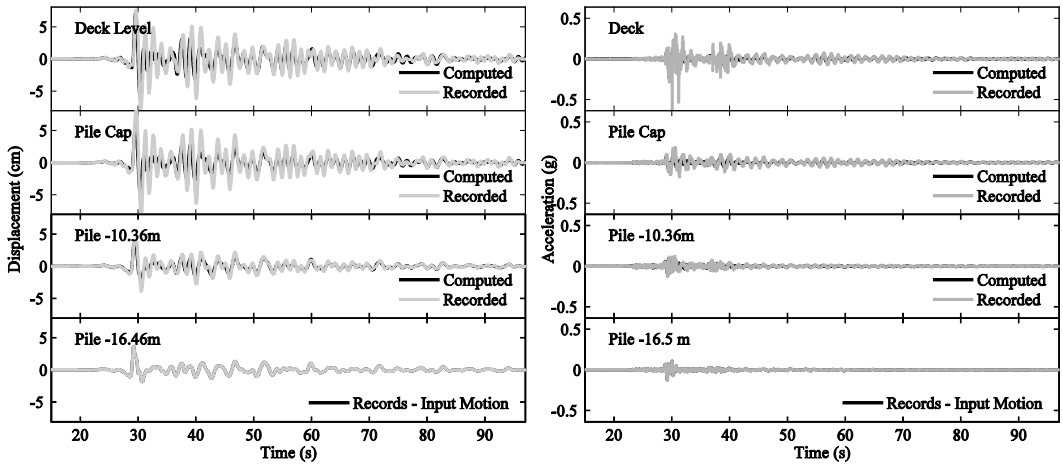

Figure 4.3: Time histories comparisons along Pier S-8 from deck level to elevation of -16.46 m during the moderate event

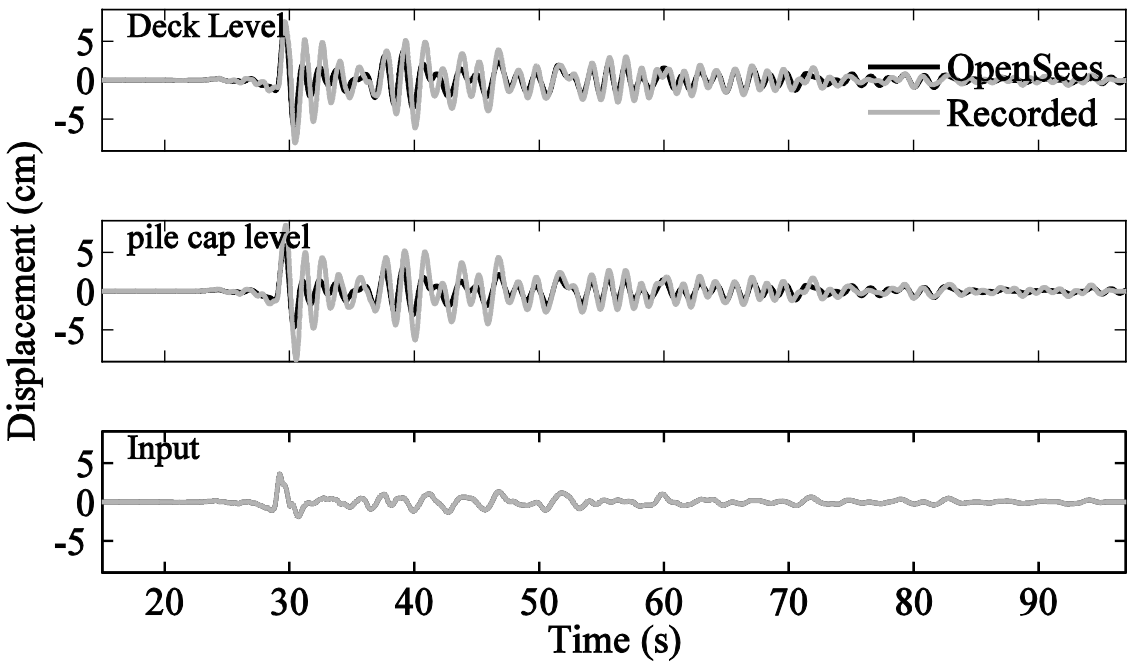

(a)

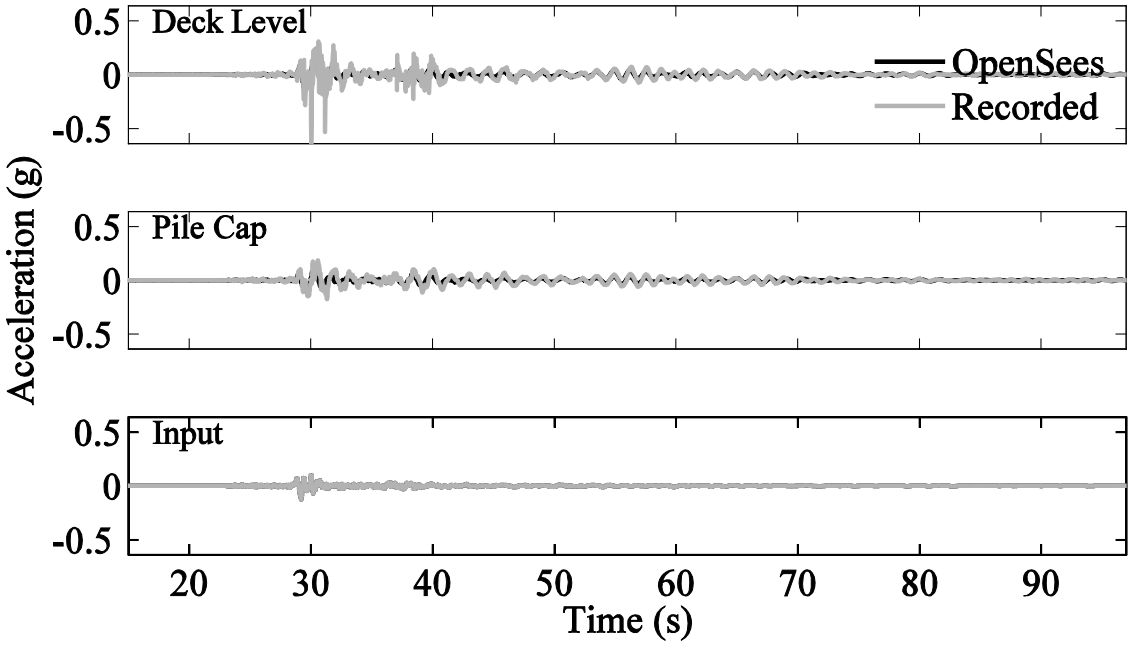

(b)

Figure 4.4: The recorded and computed time histories (FE model with base spring at Pier S-8)

5 Recorded Seismic Response and Numerical Analysis of the Eureka Channel Bridge

5.1 Introduction

In this section, data from the extensively instrumented Eureka Channel Bridge and the Eureka geotechnical downhole array (Figure 5.1) are employed to elucidate the structure seismic response (including ground, pile foundation, and super-structure). Time histories, frequency spectra and system identification analyses are presented for assessment of the ground-foundation-bridge response mechanisms. Additional sets of recorded low amplitude seismic motions are studied as well for comparison. Motions at the bridge free fields (Samoa Channel Bridge, Middle Channel Bridge and Eureka Channel Bridge), deeply embedded pile below Pier E-7 and the nearby free-field geotechnical array (Eureka Geotechnical Array) are compared and discussed in detail.

On this basis, a linear FE model representing the instrumented Eureka Channel Bridge Pier E-7 and its pile group foundation is developed and calibrated. To maintain focus, attention is directed to the bridge transverse response. The representative stiffness for the pier column and the pile foundation beneath is estimated by matching the computed dominant natural frequency of the model with the identified values.

Furthermore, the spring value representing the effects of the soil-foundation system below pier E-7 is identified. This calibrated FE model is found to mimic the seismic response of the bridge and yield comparable results with the recorded earthquake strong motion data.

5.2 General Bridge Information

5.2.1 The Bridge Description

The Eureka Channel Bridge connecting Eureka and Woodley Island (Figure 5.1) is one of three bridges crossing Humboldt Bay in Eureka, California. This 15-span bridge is a 553.44 m long and 10.36 m wide structure, supported by 14 single hexagonal concrete column type piers and seat-type abutments (Figure 5.2). The bridge piers are labeled from Eureka to Samoa as Pier E-1 (abutment), Pier E-2, Pier E-3 and so on. This bridge includes a curved section (Figure 5.2) with a radius of 548.64 m for a total length of 309.15 m from Pier E-1 up to 11.677 m NW of Pier E-9.

The continuous cast-in-place (CIP) pre-stressed (PS) 3-cell box girder superstructure is resting on reinforced concrete (RC) "T" piers from E- 1 to E-3. Four PS RC I-girders along with CIP concrete slabs (0.165 m in thickness) are supported on the hammer head of column type piers from E- 4 to E-15 and the RC seat-type abutments E-16. Between Pier E-7 and Pier E-8, there is a 42.67 m long prestressed precast concrete drop-in span. Seven separation joints allowing movement during seismic events are located at the top of Piers E-3, E-4, E-6, E-9, E-13 and the two abutment supports (Figure 5.2).

The height of the single hexagonal concrete pier columns ranges from 2.39 m at Pier E-15 to 12.25 m at Pier E-6. The abutments and pier columns are founded on pile-groups consisting of driven pre-cast prestressed concrete piles. Referenced to the mean sea level (MSL), the mudline elevation varies from +2.8 m at Pier E-3 to a -5.0 m at Pier E-8. Nearly all pile caps are embedded in soil except for pile caps from E-7 to E-10 which are around 7.35 m – 8.35 m above the mudline (Figure 5.2).

When designed in 1968, pile groups under the main span (below Pier E-7 and Pier E-8) consisted of 8 (2x4) cylindrical (diameter D=1.37 m) concrete piles (filled with concrete for it entire length) with center to center spacing of 2D. The foundation of Piers E-9 and E-10 consists of five RC piles with a RC skirt. At the reinforced concrete seat type abutments E-1 and E-16, there are 12 square-shaped concrete pile (d=35.6 cm). The front row consists of 8/7 piles battered at a 1:3 ratio and the back row consists of 4/5 vertical piles. Detailed design drawings along with soil borings are reported by Caltrans (Caltrans 2002b).

5.2.2 Site Description

Thirteen borings were drilled to a maximum depth of about 37.19 m below the mean sea level (MSL) along HWY 255 in 1968 (Figure 5.3). It is revealed that the bridge site is mantled by very soft silty clay underlain by dense gray medium to compact gray sand. Stiff grey was encountered at the elevation of -12.2 m and continues to the maximum explored depth. Soil layers vary in thickness and are not continuous horizontally (Caltrans 2002b).

5.2.3 Seismic Retrofit Effort

The Eureka Channel Bridge was designed by the California Department of Transportation (Caltrans) in 1968 and the construction was completed in 1971. Minor damage was reported after earthquakes in 1992 and 1994. Some repairs and subsequently an initial seismic retrofit (Caltrans 2002b) were completed by Caltrans prior to 1997 (e.g., the bent caps were reinforced and transversely stressed; pipe extenders and cable assemblies were added to selected bents, etc.).

In order to further strengthen this bridge, a seismic retrofit program was carried out by Caltrans in 2002, which included (Caltrans 2002b): (1) strengthening of the foundations by

installing additional cast-in-steel shell (CISS) piles (e.g. 2 additional 0.914 m diameter and 13 mm thickness piles at both noses of the pier footings from Pier E-7 through E-10, as shown in Figure 5.4); (2) adding or enlarging pile caps to cover the new piles. The original skirt was retained at each pier. The retrofit skirt extended through the overall length of the pier but retained the original width; and (3) encasing the bridge columns in reinforced concrete column jackets to improve ductility. Accelerometers were installed inside one of the Pier E-7 retrofitted CISS piles at two different elevations (-10.36 m and -16.46 m) during the structural retrofit. Detailed design drawings, retrofit information along with soil borings are reported by Caltrans (Caltrans 1968; Caltrans 2002b).

5.3 Strong-Motion Instrumentations at the Eureka Channel Bridge

5.3.1 Instrumentations of the Eureka Channel Bridge

The Eureka Channel Bridge was heavily instrumented (CGS station 89736) with a total of 27 accelerometers (mostly deployed in 1996). Side view and deck level plan view of the sensor network layout are shown in Figure 5.2. Locations of sensors are marked with numbered arrows indicating the direction of measured motion.

There are 18 sensors placed on the Eureka Channel Bridge to measure the translational motion of the structure, including 10 on the deck, 3 at the abutments and 5 at the pile caps of Pier E-3 and Pier E-7 (Figure 5.2). Sensors on the structure are oriented in the longitudinal and transverse direction of the bridge (positive direction of transverse motion defined as radially inward for this curved bridge). At a nearby ground surface station (EGS, 33.53 m south of the Abutment E-1 and 7.62 m west of E-1), three sensors were installed at elevation of +1.9 m approximately, oriented in the north-south (NS), east-west (EW) and vertical directions (Figure

5.2). In addition, 6 accelerometers were embedded inside one of the retrofitted CISS piles at Pier E-7 (Figure 5.4). Foundation seismic response at two different elevations (-10.36 m and -16.46 m) was included after the structural retrofit.

5.3.2 Recorded Earthquake Motions

Records from a total of nine earthquakes (Table 5.1) in the period of June 2002 through March 2014 are currently available with Magnitudes from 4.5 M_L to 7.2 M_W (M_L: local magnitude and Mw: regional moment magnitude). Notable in Table 5.1 is the 2010 Ferndale Earthquake (M_w of 6.5) which is the first significant earthquake data set obtained since the retrofit in 2002 and is the largest motion recorded on the bridge. The bridge at a distance of 54.5 km from the epicenter of this earthquake reached peak acceleration of the order of 0.26 g at the ground surface and 0.51 g on the bridge deck. The largest movement on the bridge structure was 6.8 cm longitudinally and 6.1 cm transversely referenced to the motions of the pile at -16.46 m depth (Figure 5.4) during this earthquake event.

5.4 Evaluation of Earthquake Records

5.4.1 Ground Motions at the Bridge and Adjacent Downhole Sites

Comparison of the ground surface motions at three Caltrans bridge sites: the Samoa Channel Bridge (SCB), the Middle Channel Bridge (MCB), and the Eureka Channel Bridge (ECB) crossing the Humboldt Bay and at the Eureka Geotechnical Downhole Array (GDA) is shown in Figure 5.5. Synchronization between the bridges and GDA records was done based on the actual digital time stamp for each site. In addition, arrival time of the ground surface seismic waves at the GDA and bridge sites differed by less than 0.2 second as judged by cross-

correlation analysis. Overall, the ground surface displacement responses are of the same pattern (Figure 5.5). Generally, Fourier transformations of the acceleration time histories indicate the same dominant frequencies (Figure 5.6).

Figure 5.7 present ground displacement of: 1) the Eureka Channel Bridge ground surface station (EBGS), 2) the Eureka Channel Bridge pile foundation (EBPF) at the elevation of -16.46 m (re-oriented based on cross-correlation calculation as described in section 5.4.3), and 3) the adjacent geotechnical downhole array (GDA) in EW and NS directions.

As may be noted, motions at the EBGS and the EBPF (estimated at about 12.46 m below the mudline at this location) are of the same pattern as that of the GDA stations (being somewhere between the ground surface and elevation of -16 m). The pseudo-acceleration response spectra, with 5% damping, for the recorded free field motions of the bridge as well as those of the adjacent downhole array are shown in Figure 5.8 for the moderate event. There is a noticeable amplification effect for the motion at the downhole ground surface compared to those at depth. In particular, spectral acceleration of the EBPF falls between those of downhole at the ground surface and 33 m depth in the short period range. It is noteworthy that the pseudo-acceleration of the bridge at the ground surface station is significantly high at low period. This observed high energy response at low period might be partly due to the soil profile characteristics at the site and partly due to the impact of the bridge.

Generally, the location of -16.46 m along the pile depth will be assumed to be practically moving along with the ground (Figure 5.7), indicating a level of firm embedment (fixity). Similar conclusions can be obtained based on comparisons of records from other available low amplitude earthquakes.

5.4.2 Seismic Response along the Bridge Deck

As shown in Figure 5.9b - Figure 5.10b, relative displacement time histories (referenced to the motions at EBPF station) generally display in-phase behavior in both directions (Transverse defined as radially inward for this curved bridge) for the moderate earthquake events. Overall, the bridge is noticeably flexible in the mid-span (Channels 4 and 5 at Pier E-7). For the moderate event, maximum relative displacement at pier E-7 is 60% larger in amplitude compared to that at the abutment (E-16) in the transverse direction. In addition, relative displacement time histories highlight the period of vibration in both translational directions for this curved bridge during the low amplitude shaking events.

Sharp spikes were observed from the deck acceleration time histories in the translational directions (Long and Tran directions) for the moderate event (Figure 5.10a). Among these, the highest spike is 0.95 g at Chan4 in the longitudinal direction and 0.51 g at Chan19 in the transversal direction, whereas the peak ground acceleration at the bridge site is only about 0.26 g (Table 5.1). Such spikes were likely caused by a head-on impact between adjacent bridge deck segments (Huang and Shakal 1995; Malhotra et al. 1995). No spikes were observed during the low amplitude shaking event.

5.4.3 Seismic Response of Pier E-7

Given the discontinuity of the bridge structure due to the existence of separation joints near Pier E-7, transverse motion of the central intermediate bent may be analyzed individually (in an approximate manner, independent of the rest of the bridge). In addition, the high translational motion observed at Pier E-7 near the mid-length of the bridge, indicates that this might be a vulnerable location of the bridge. Of particular interest in this study was the dynamic

response of the bridge structure relative to the pile foundation in the transverse direction at the mid-span Pier E-7.

Due to the uncertainty of sensor orientations within the retrofitted pile, cross-correlation analyses were performed to check for potential azimuthal error. It was found that sensors at the elevation of -16.46 m need to be rotated 8.5 degrees (clockwise) based on cross-correlation between the EBGS motion and the EBPF responses. For the sensors at elevation of -10.36 m, 22.1 degrees rotation is needed for the highest correlation with the recorded pile cap response.

As such, based on comparisons of the displacement time histories (Figure 5.11 and Figure 5.12), it can be concluded that the pile cap and bridge deck displacements are noticeably different. Relative displacement time histories during the low amplitude shanking event (the 2007 Ferndale Earthquake) show a clear dominant fundamental response period. The bridge transverse displacements are due to deformation of the pile and the pier as well (Figure 5.13 and Figure 5.14). More bridge displacements at pier E-7 during recorded earthquakes are shown in Wang (2015).

5.4.4 Abutment and Bridge Response along Mudline

Figure 5.15 and Figure 5.16 compare the acceleration and displacement time histories of bridge base along the ground surface (including motions at the EBGS, the EBPF, on the pile cap near ground surface and at the bridge abutments). It was observed that displacement time histories are of the similar pattern. In the longitudinal direction, spikes were observed at the abutment and on the pile cap of Pier E-3 during the moderate event. All these observations indicate that the motions recorded on the E-3 pier footing, on the pile at elevation of -10.36 m and on the abutment of Pier E-16 are affected by the bridge response. For this curved bridge,

motions recorded at the ground surface and at the EBPF (-16.46 m below MSL) can potentially be used as input excitation for general numerical modeling procedures.

5.5 System Identification for the Ground-Foundation-Bridge System

The Transfer Function approach (TF) is employed to assess the system and sub-system resonant frequencies. In the transverse direction, the fundamental frequency for Deck-Pier sub-system (deck response referenced to pile cap response) at Pier E-7 is in range of 2.42-2.54 Hz for the low amplitude earthquakes. The same logic is then employed to relate the deck response to that of the pile at -16.46 m (taken here to be the fixed base), and also related to the nearby free-field ground surface motion. A Hanning window and 50% overlap is adopted to reduce the effects of spectral leakage. The first natural frequency for this bent of the bridge system was found to be around 1.5 Hz during these low amplitude earthquakes. A summary of the TF results for 4 low amplitude earthquakes is presented in Table 5.2 and Table 5.3.

5.6 Finite Element Analysis

5.6.1 Finite Element Modeling

Based on time history data analysis, Pier E-7 could be considered, in an approximate manner, to move independently of the influence of the rest of the bridge (in the transverse direction). A linear elastic OpenSees FE model of Pier E-7 (including the deck, the Pier, and the pile group below) is developed based on the “as-built” geometry of the bridge and updated with column/pile foundation stiffness based on the identified characteristics. This model consisting of point masses at the bridge deck level and the pile cap level is connected by linear elastic beam-column elements. With the aid of the identification techniques, an attempt is made to demonstrate variations of flexibilities for the ground-foundation system. In particular, valuable

insights can be gained about: (i) nonlinear stiffness reduction levels for the column, (ii) nonlinear stiffness reduction levels for the foundation, and (iii) equivalent base spring to represent the ground-foundation system below Pier E-7.

5.6.2 Structural Modeling of the Column at Pier E-7

The bridge column at Pier E-7 was modeled with elastic beam-column elements. Center-to-center mass of the bridge deck above E-7 (including mass of deck, longitudinal I-girder and transversal beams), mass of the hammerhead column top and half mass of the column is defined as the point mass at the center of gravity for the Deck-Girder system. Calculations of masses were based on the density and volume of structural components. Since seismic motion at the pile cap level is known from the records (Channel 3), boundary condition at the base of the column is considered to be fixed in all DOFs with this prescribed motion time history.

The following material parameters were used for this idealized FE model (Caltrans 2002b): reinforced concrete mass density ρ= 2560 kg/m3, Young's modulus E=2.51x10^7 kPa (compressive strength $f_c' = 28\text{MPa}$) for existing reinforced concrete and Young's modulus E=2.39x10^7 kPa (compressive strength $f_c' = 25\text{MPa}$) for retrofit reinforced concrete, Poisson's ratio ν=0.2 for concrete and Young's modulus E_s=2.0x10^8 kPa for steel.

For the FE analysis, gross moment of inertia for the concrete column based on the uncracked section is employed. Flexural stiffness (EI) of the connecting bending beams is then calibrated through eigenvalue analysis to match the identified bridge-bent resonant frequencies in Table 5.2. The pier column stiffness (Table 5.4) appears to be noticeably smaller than calculations might imply (about 61% of the gross EI is engaged). It agrees well with the common Caltrans practice where effective moment of inertia is the range between gross and cracked moment of inertia (Caltrans 2012; Caltrans 2013). As such, the calibrated pier stiffness includes

contributions from interaction (resistance) due to the overall bridge connectivity. It is noted here that no recorded deck motion was available for the moderate event, which did not permit for conducting a similar analysis.

5.6.3 Structural Modeling of the Pile Foundation below Pier E-7

Center-to-center mass of the bridge deck above E-7 (including mass of deck, longitudinal I-girder and transversal beams), mass of the hammerhead column top and half mass of the column is defined as the 1st point mass at the center of gravity for the Deck-Girder system. Half mass of the column, mass of the pile cap, and half mass of the pile groups is lumped at the elevation of the pile cap level (2nd point mass). As presented earlier, seismic motion at the pile -16.46 m below the mean sea level is known from the records (Chan 27). Base boundary condition for the pile foundation is considered to be fixed in all DOFs with prescribed motion time history at this location. The pile cap mass location was assumed to be fixed against rotation (due to the spatial extent of the underlying pile group).

The pier column and pile foundation (taken as a single equivalent super-pile with the union of the cross section of all the piles) is modeled with linear beam-column elements. A large EI is set for the element representing the pile cap in order to achieve rigidity.

Based on eigenvalue analysis, one might calibrate the pile group foundation lateral stiffness to match with the identified bridge resonant frequency. It turns out that the employed quantities amounted to a factor of about 3.0 for the stiffness of pile group foundation (Table 5.5 low amplitude earthquakes). This stiffness for the pile might be reasonable considering the support provided by the surrounding soil. Unlike the Samoa Channel Bridge, most of pile foundation below Pier E-7 is embedded in the ground. It is noted here that no recorded deck

motion was available for the moderate event, which did not permit for conducting a similar analysis.

Computational simulation results show a reasonable match from the pile cap to the deck (column part, Figure 5.17) and from the base to the deck (Figure 5.18). As such, the calibrated stiffness includes contributions from interaction (resistance) due to the overall bridge connectivity, and the pile foundation lateral stiffness implicitly accounts for SSI.

5.6.4 Modeling of Base Springs

Linear lateral springs were attached to the base of superstructure (at the pile cap location) to account for stiffness of the underlying pile foundations and the soil-foundation-structure interaction. Recorded motion at -16.46 m of the retrofitted pile is employed as the uniform base dynamic excitation at the ends of springs along the bridge length. Base springs representing the stiffness of the pile foundation at pier E-7 in the local transverse direction is identified (Table 5.8) for low amplitude shaking events. To this end, the FE model for the isolated Pier E-7 with identified spring value provided a good match with the recorded pier response (Figure 5.20).

Overall, it is found that computed response of the bridge model is in good agreement with the recorded motions at various locations of the bridge.

5.7 Conclusions

In this section, a comparison of the measured displacement time-history records indicated that: (1) unlike seismic response of the Samoa Channel Bridge, the relative displacement between the top and bottom of Pier E-7 is noticeable indicating a relatively stiffer pile group behavior, (2) displacement time histories at ground surface and at the -16.46 m depth location of the pile followed similar wave patterns.

An OpenSees FE model of the bridge pier column was developed and calibrated based on the observed seismic response. Computed bridge response was generally comparable to the actual measurement in the time domain indicating that the adopted strong motion data analysis techniques have captured salient seismic characteristics and are helpful for calibration of the FE model.

Table 5.1: Recorded peak acceleration for recent earthquakes at the Bridge Site (arranged by order of peak acceleration)

Earthquake	Magnitude	Epicentral Distance (km)	Horiz. Peak Acc. (g)	
			Ground	Structure
Ferndale Jan 09, 2010	6.5 (M_w)	54.5	0.256	0.510
Ferndale Mar 09, 2014	6.8 (M_w)	82.6	0.027	0.072
Trinidad August 16, 2008	4.6 (M_w)	41.7	0.022	0.061
Humboldt Hill August 02, 2013	4.5 (M_L)	20.8	0.022	0.022
Trinidad June 24, 2007	5.1 (M_L)	65.6	0.020	0.081
Ferndale February 04, 2010	5.9 (M_w)	77.8	0.018	0.046
Willow Creek April 29, 2008	5.4 (M_w)	55.4	0.012	0.026
Ferndale February 26, 2007	5.4 (M_L)	63.2	0.011	0.021
Crescent City June 14, 2005	7.2 (M_L)	155.1	0.006	0.021

Table 5.2: Identified resonant frequency of bridge pier in the transverse direction

EQ	Fundamental Frequency (Hz) in transverse direction	
	Transfer Function $\frac{\text{deck}}{\text{Pile Cap}}$	MATLAB toolbox Parametric identification
Trinidad June 24, 2007	2.49	2.22
Willow Creek April 29, 2008	2.42	2.12
Trinidad August 16, 2008	2.54	2.16
Ferndale February 26, 2007	2.50	2.22

Table 5.3: Identified resonant frequency of bridge system in the transverse direction

EQ	Fundamental Frequency (Hz) in transverse direction		
	Transfer Function $\frac{\text{Deck}}{-16.46\text{ m}}$	Transfer Function $\frac{\text{Deck}}{\text{free field}}$	MATLAB toolbox Parametric identification
Trinidad June 24, 2007	1.52	1.52	1.59
Willow Creek April 29, 2008	1.57	1.43	1.56
Trinidad August 16, 2008	1.46	1.43	1.63
Ferndale February 26, 2007	1.59	1.63	1.59

Table 5.4: Identified frequency and stiffness factor for pier at Pier E-7 based on uncracked section

Earthquake Event	Frequency (Hz)	Column Stiffness Factor
Trinidad June 24, 2007	2.49	0.61
Willow Creek April 29, 2008	2.43	0.58
Trinidad August 16, 2008	2.53	0.63
Ferndale February 26, 2007	2.49	0.61

Table 5.5: Identified spring value representing pile foundation below Pier E-7

Earthquake	Identified frequency (Hz)	Identified stiffness factor for pile group
Trinidad June 24, 2007	1.52	2.97
Willow Creek April 29, 2008	1.57	3.25
Trinidad August 16, 2008	1.46	2.65
Ferndale February 26, 2007	1.59	3.35

Table 5.6: Uncracked section properties for pier column S-8 (Caltrans 2002b)

Uncracked section	Pier E-7
Area of Cross Section	7.01 m^2
Transverse Moment of Inertia	7.06 m^4
Longitudinal Moment of Inertia	1.88 m^4
Torsion Constant	5.77 m^4

Table 5.7: Identified spring value representing pile foundation below Pier E-7

Earthquake	Identified spring value K (kN/m)	Computed Frequency (Hz)
Trinidad Jun 24, 2007	1.79×10^5	1.52
Ferndale Feb 26, 2007	2.05×10^5	1.59
Trinidad Aug 16, 2008	1.61×10^5	1.46
Willow Creek Apr 29, 2008	1.96×10^5	1.57

Figure 5.1: Photo of the Eureka Channel Bridge (http://www.strongmotioncenter.org)

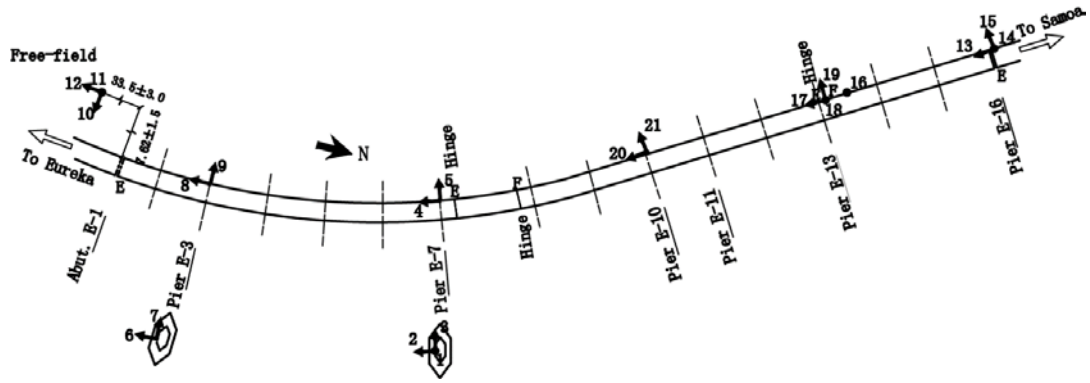

(a)

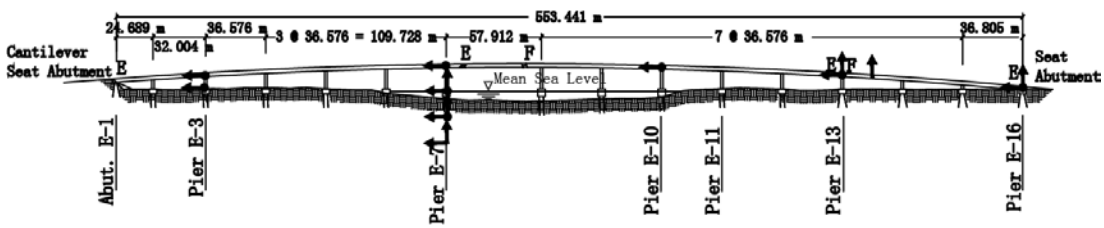

(b)

Figure 5.2: Layout of instrumentation at the Eureka Channel Bridge: (a) deck level plan and (b) elevation (http://www.strongmotioncenter.org)

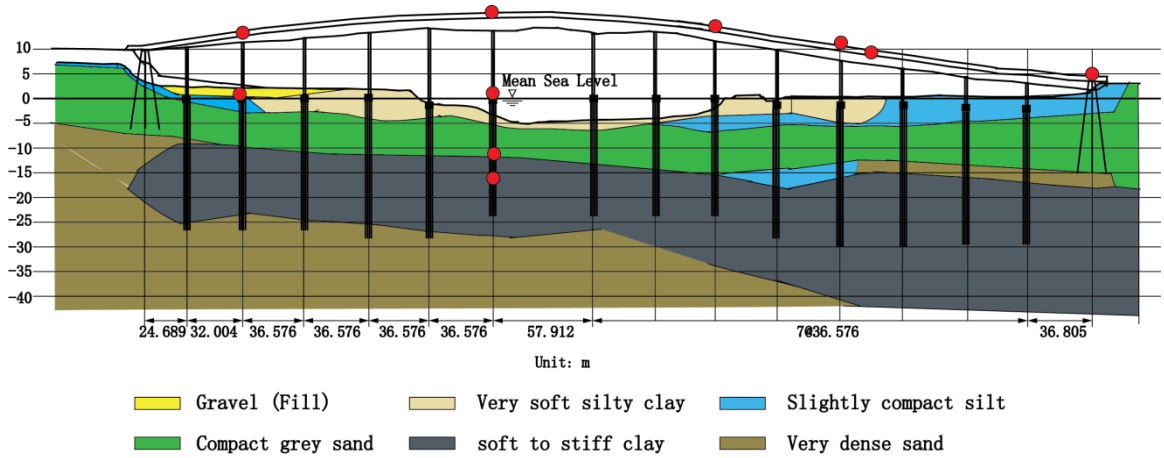

Figure 5.3: Soil Profile along the bridge (Caltrans 2002b)

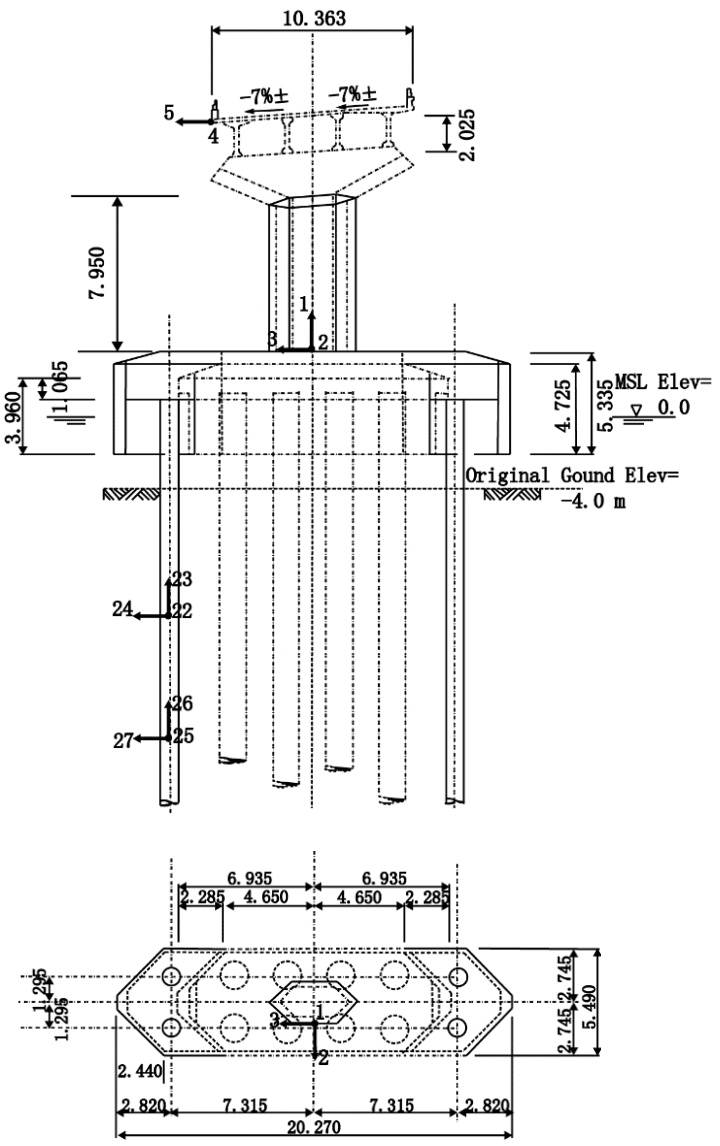

Figure 5.4: Layout of instrumentation and retrofit efforts at the Eureka Channel Bridge Pier E-7 (Caltrans 2002b)

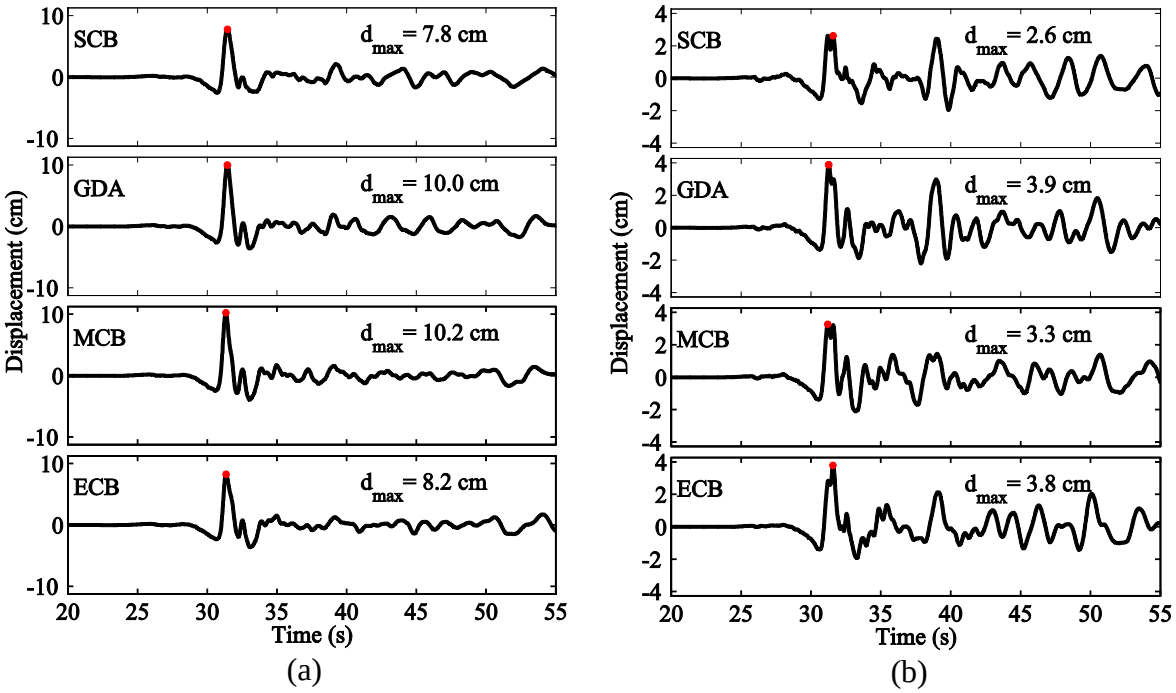

Figure 5.5: Displacements at the ground surface of the Samoa Channel Bridge (SCB), the Geotechnical downhole array (GDA), the Middle Channel Bridge (MCB) and the Eureka Channel Bridge (ECB) in the (a) NS and (b) EW directions during the moderate event

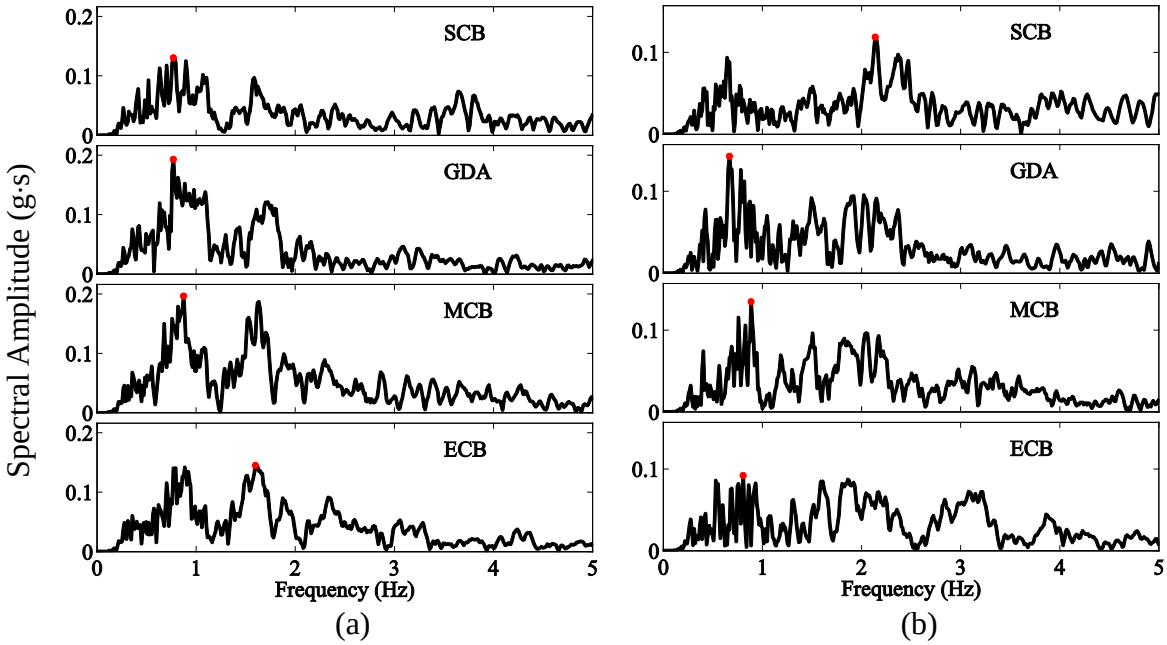

Figure 5.6: Fourier transformation of ground surface acceleration of SCB, GDA, MCB and ECB in the (a) NS and (b) EW directions during the moderate event

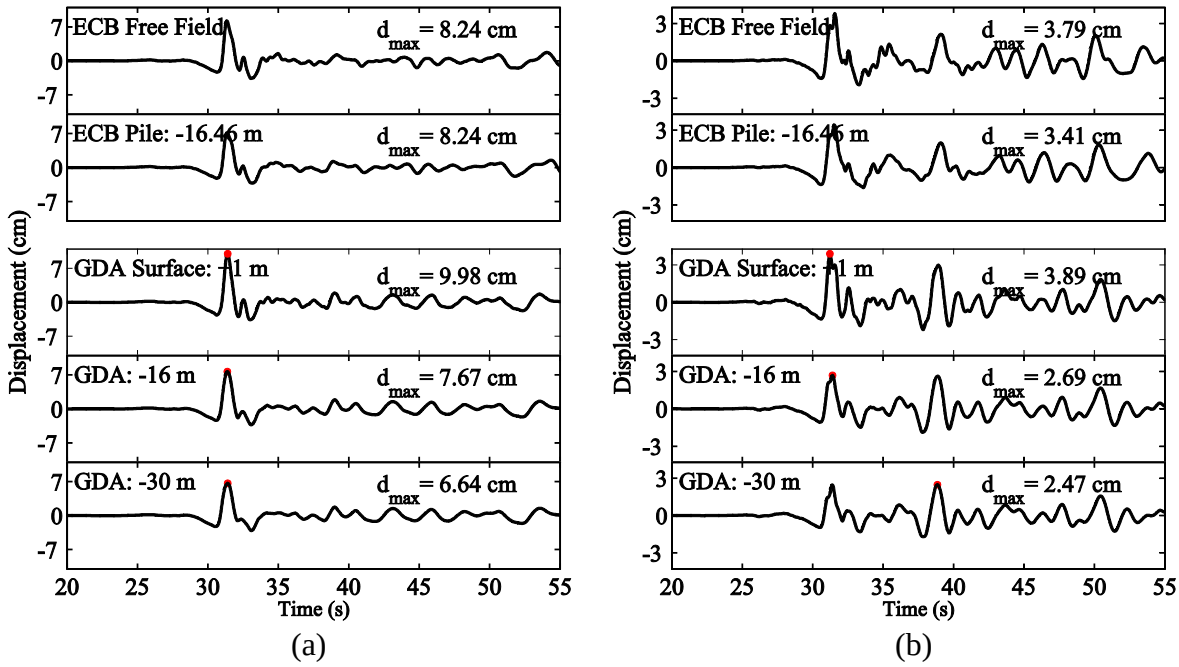

Figure 5.7: Displacement time histories in the (a) east-west (EW) and (b) north- south (NS) directions during the moderate event

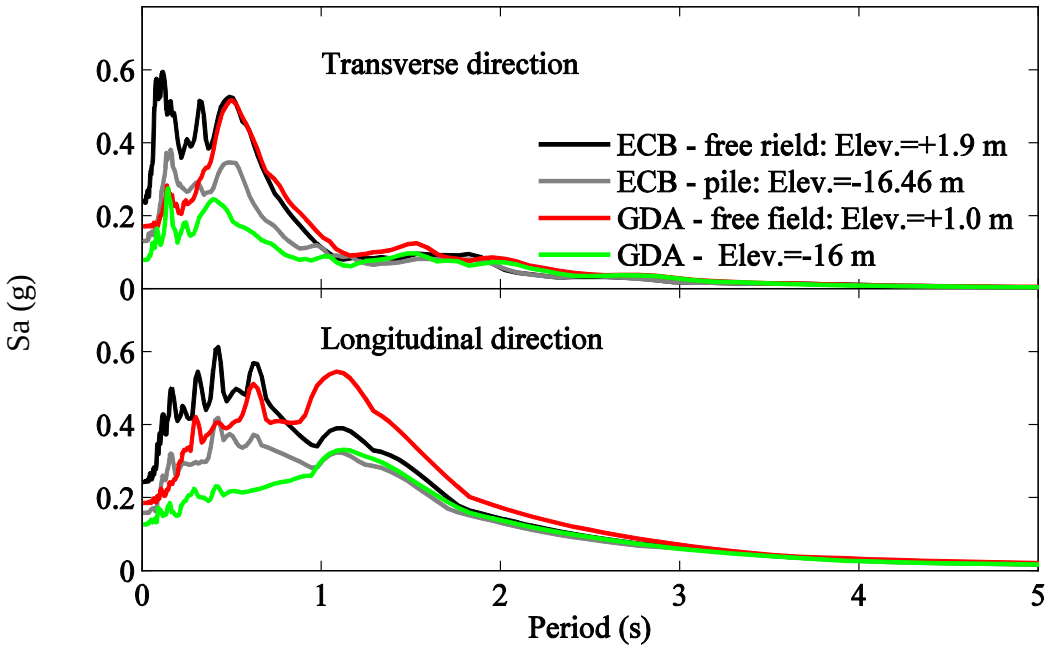

Figure 5.8: Eureka Channel bridge response spectra of free-field in the transverse and the longitudinal directions of Pier E-7 during the moderate event

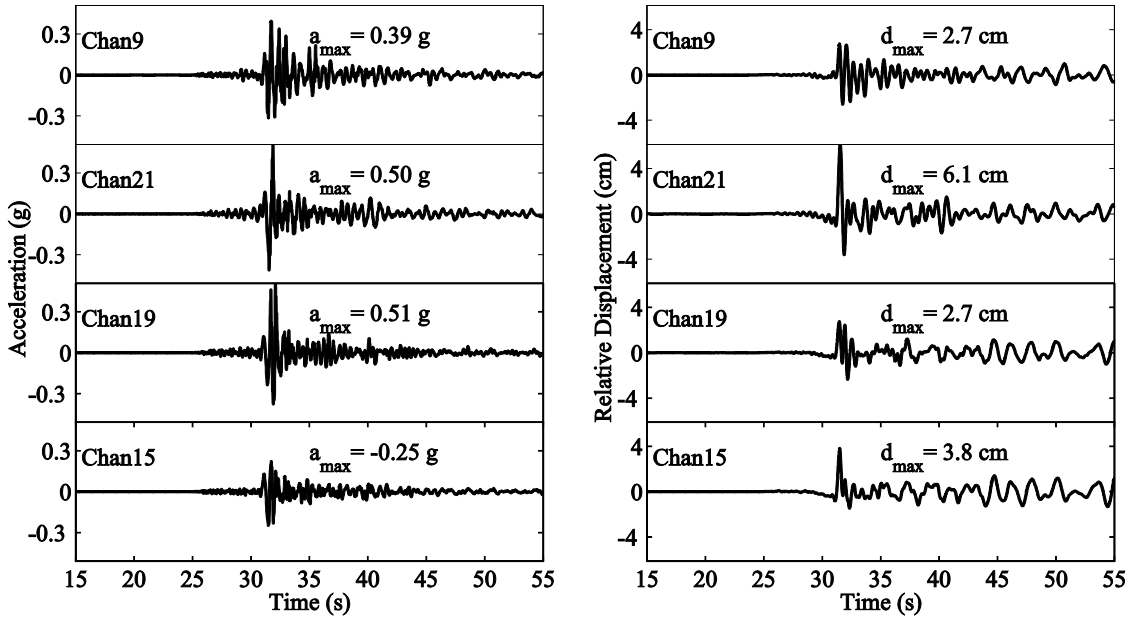

(a) (b)

Figure 5.9: Variation of time histories at bridge deck level during the moderate event for (a) acceleration and (b) relative displacement time histories (Transverse shown)

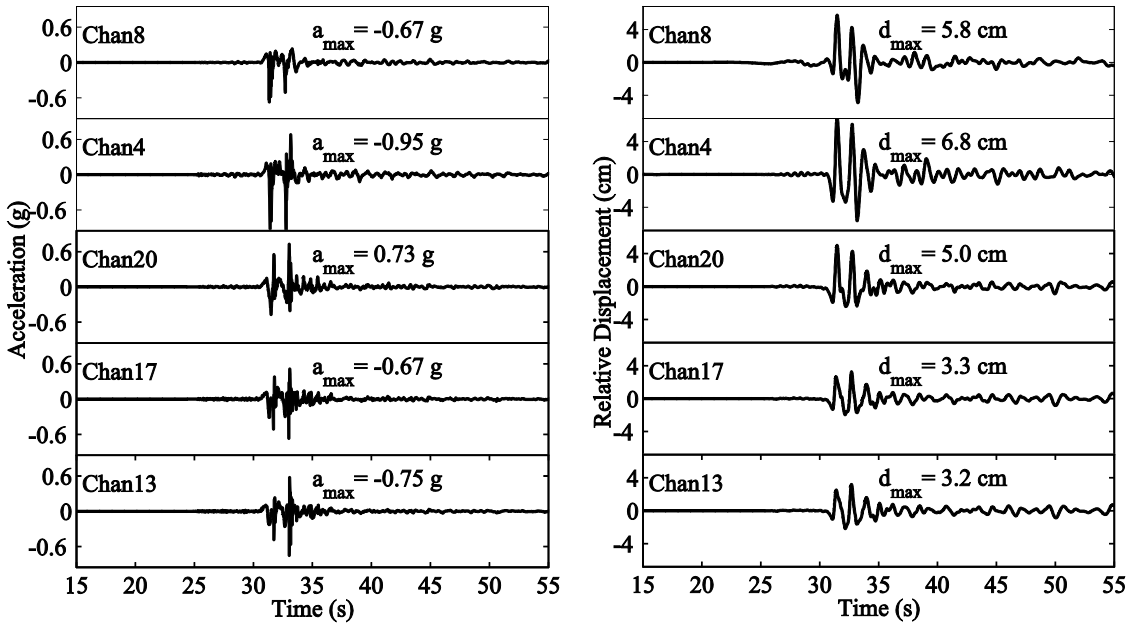

(a) (b)

Figure 5.10: Variation of time histories at bridge deck level during the moderate event for (a) acceleration and (b) relative displacement time histories (Longitudinal shown)

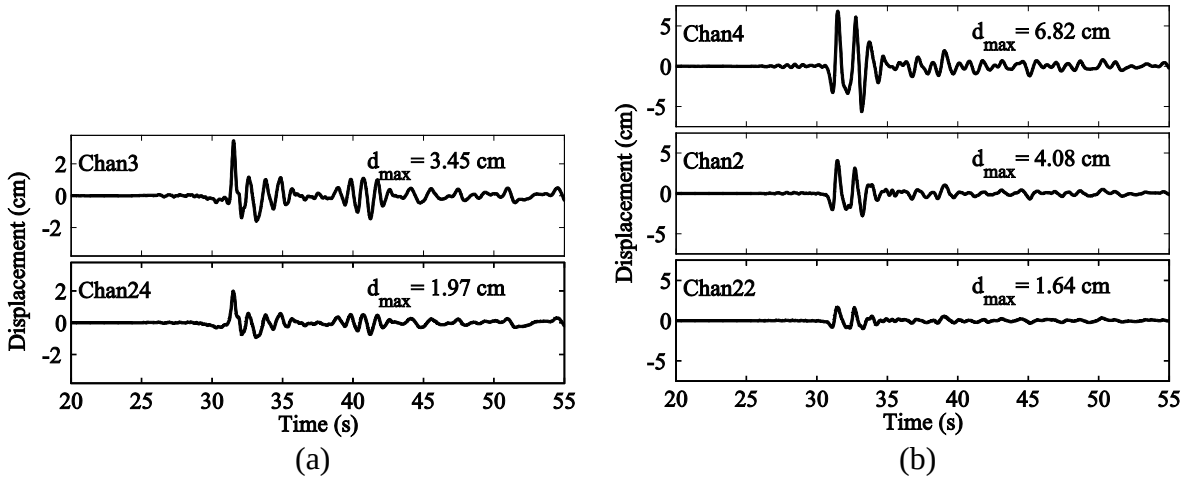

(a) (b)

Figure 5.11: Relative displacement time histories (referenced to the motions at EBPF station) along Pier E-7: (a) in the transverse direction, (b) in the longitudinal direction during the moderate event

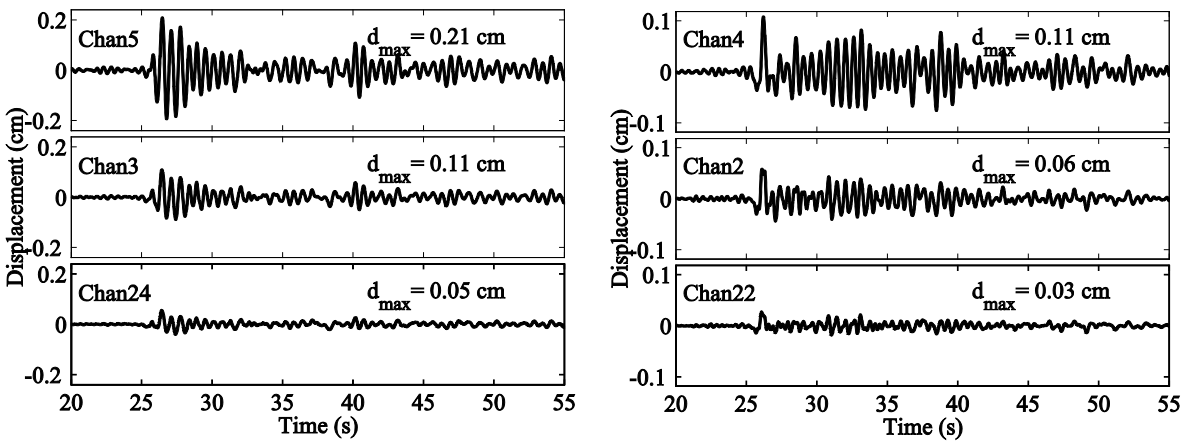

(a) (b)

Figure 5.12: Relative displacement time histories (referenced to the motions at EBPF station) along Pier E-7 during the 2007 Ferndale Earthquake: (a) Transverse and (b) Longitudinal

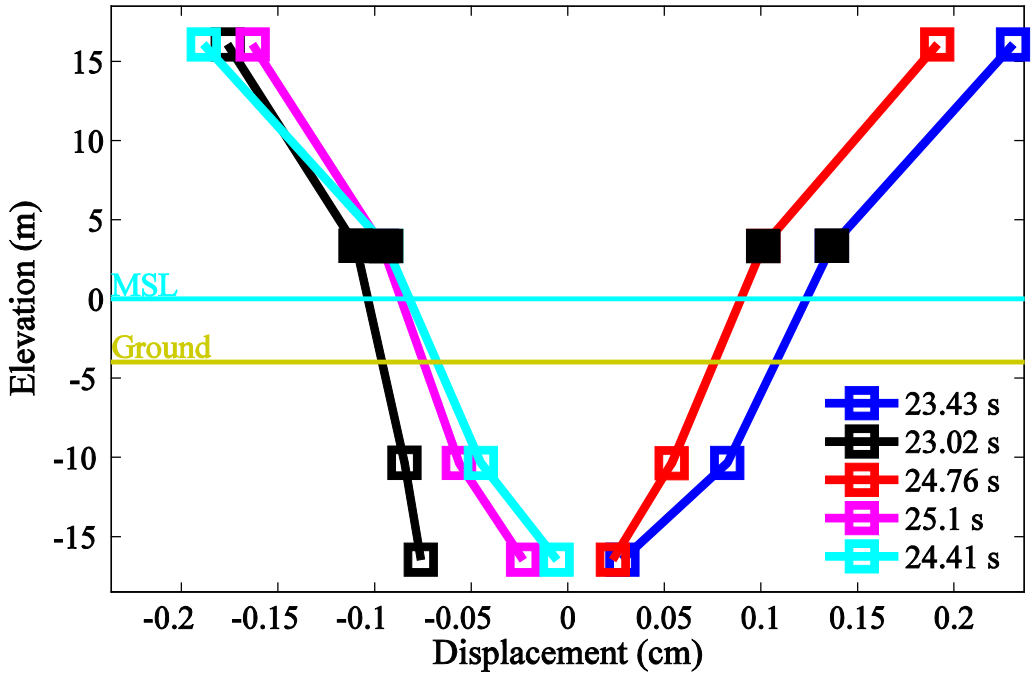

Figure 5.13: Displaced configuration of Pier E-7 for selected time instants during the 2007 Ferndale Earthquake (Transverse)

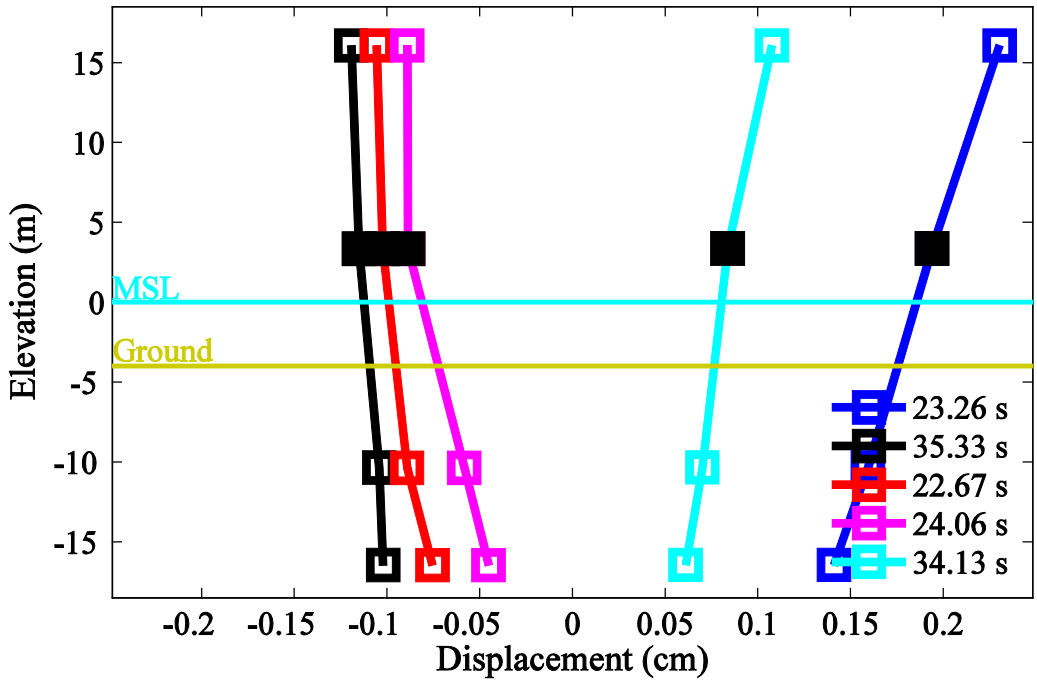

Figure 5.14: Displaced configuration of Pier E-7 for selected time instants during the 2007 Ferndale Earthquake (Longitudinal)

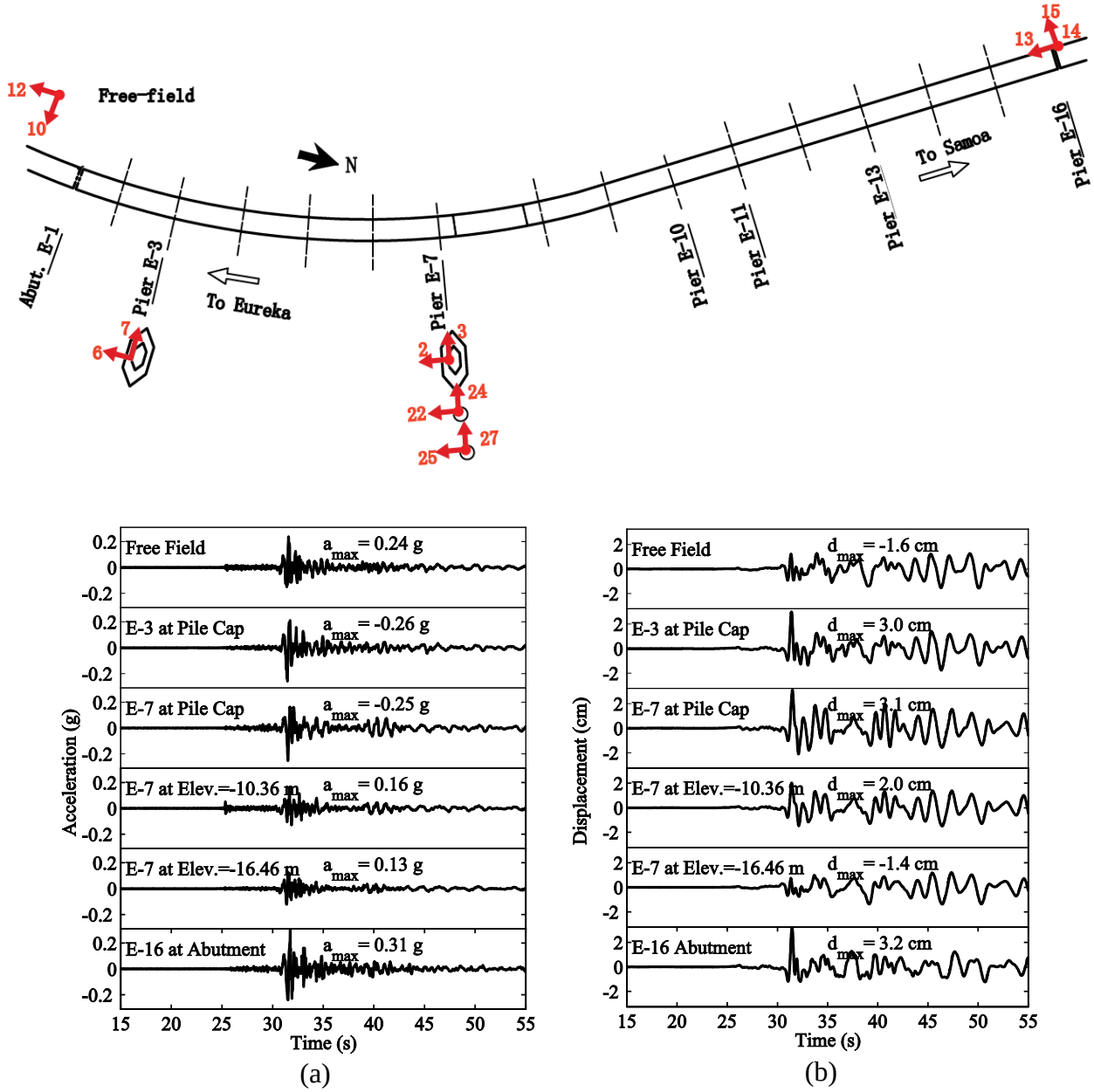

Figure 5.15: Variation of (a) acceleration and (b) displacement time histories along ground surface for the moderate event (in Tran direction of Pier E-7 shown)

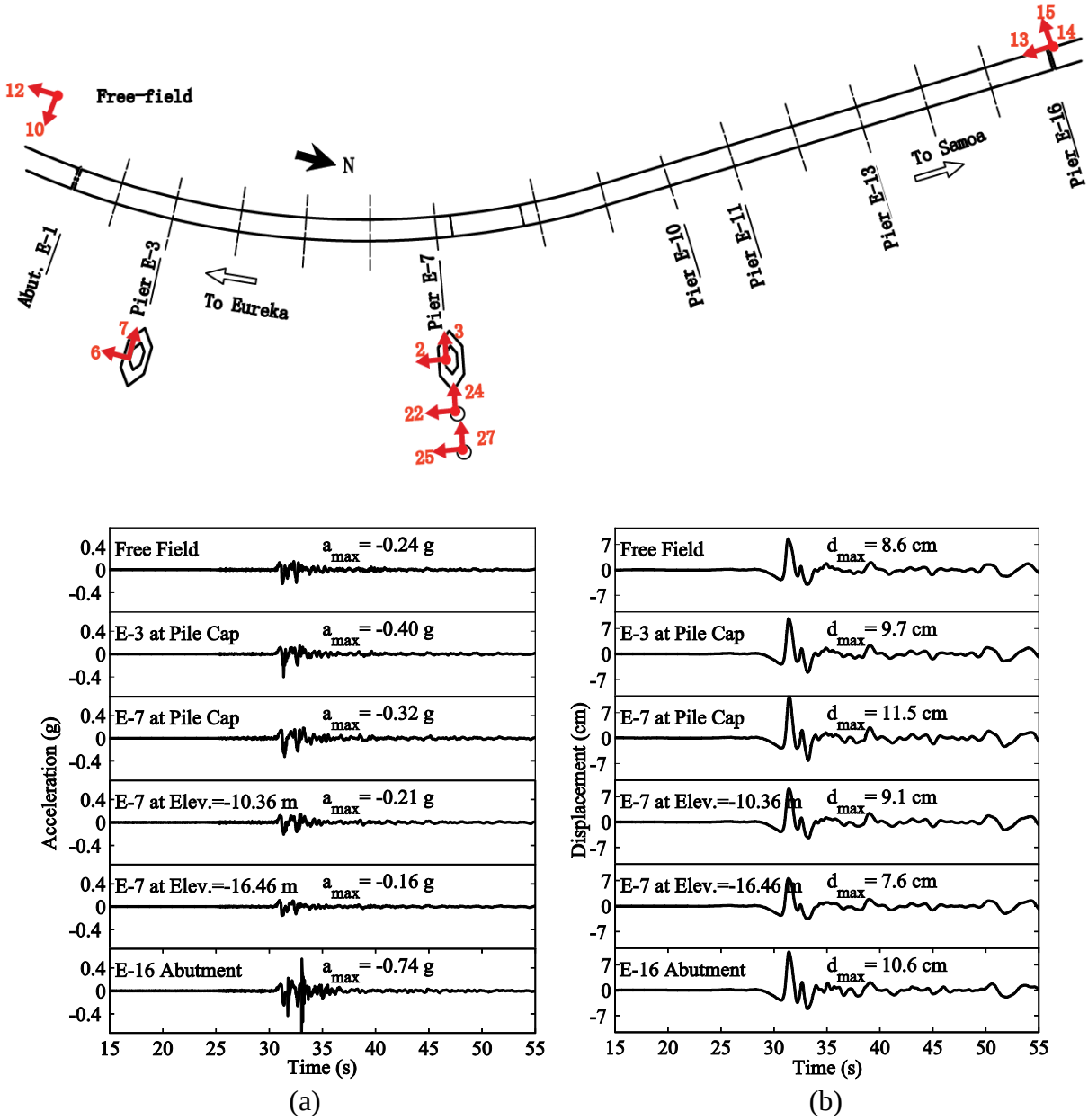

Figure 5.16: Variation of (a) acceleration and (b) displacement time histories along ground surface for the moderate event (in Long direction of Pier E-7 shown)

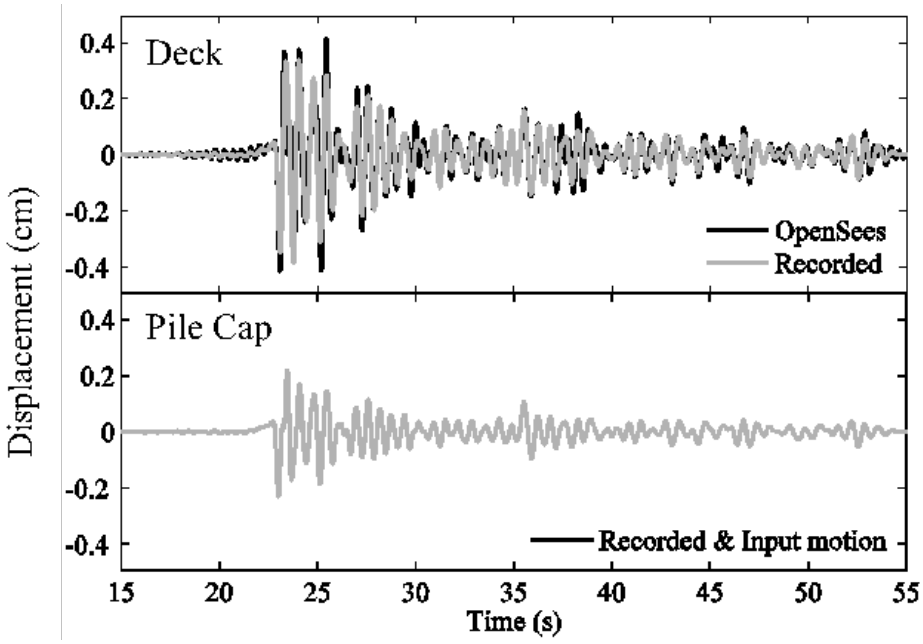

(a)

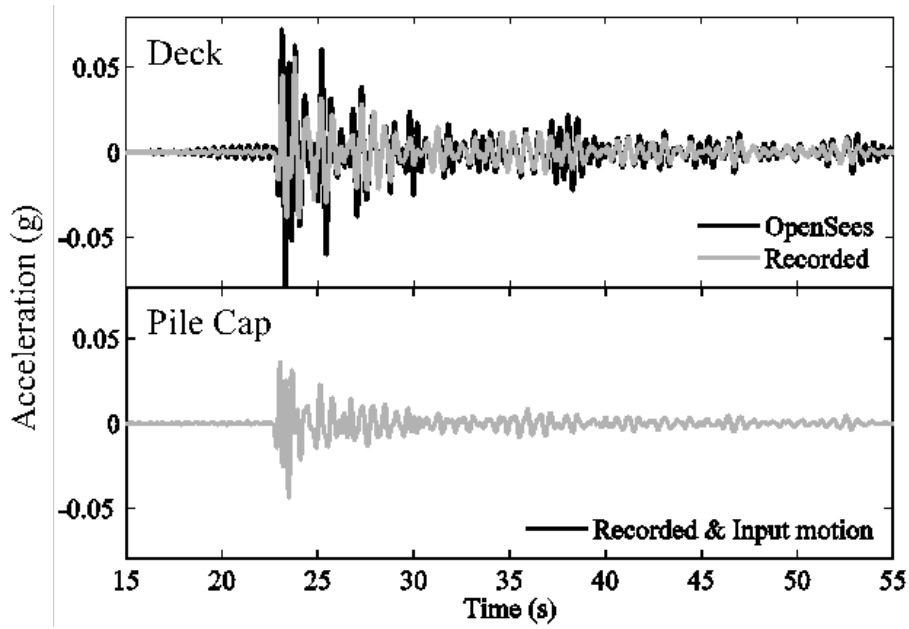

(b)

Figure 5.17: Comparison of computed and measured response at Pier E-7 during the 2007 Trinidad Earthquake

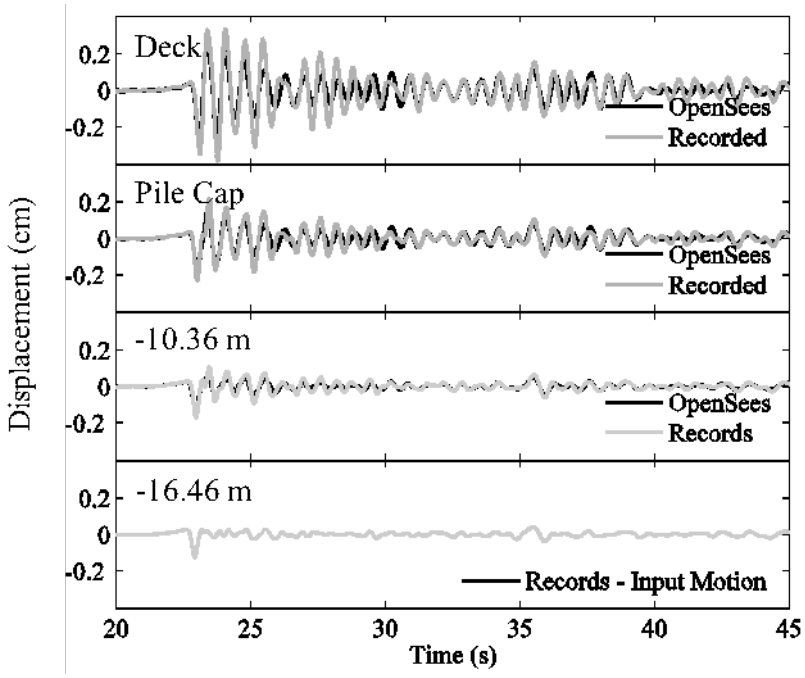

(a)

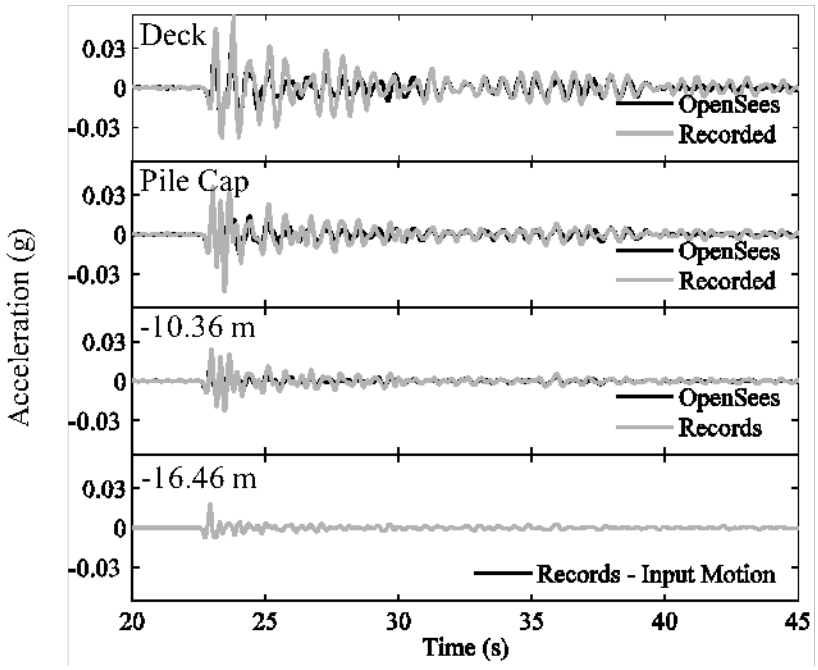

(b)

Figure 5.18: Time histories comparisons along Pier E-7 from deck level to elevation of -16.46 m during the 2007 Trinidad Earthquake

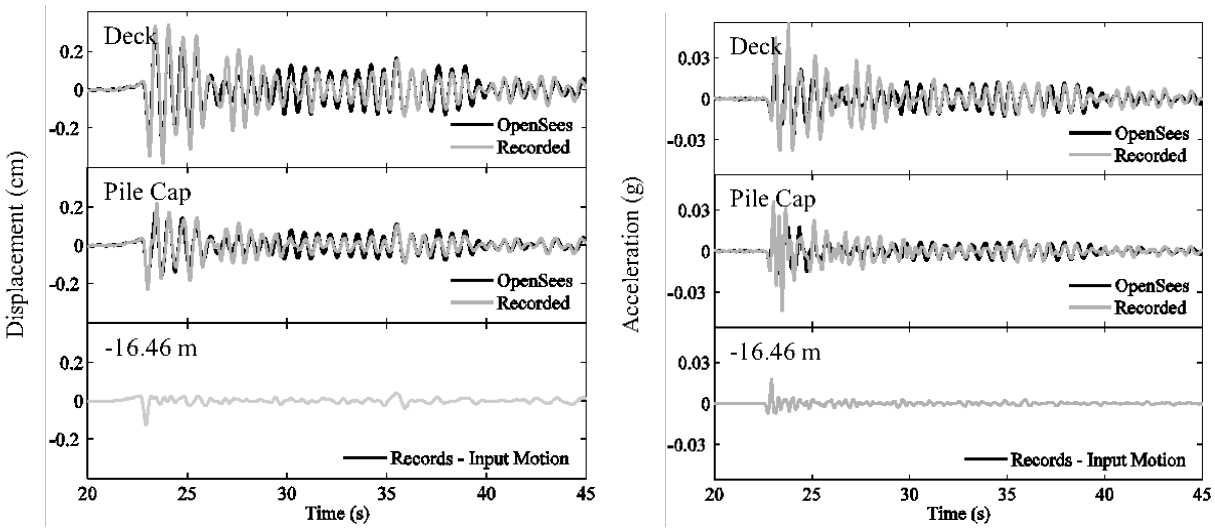

Figure 5.19: The recorded and computed time histories (with identified base spring) at Pier E-7 during the 2007 Trinidad Earthquake

6 Conclusions

Analyses of recorded earthquake response using signal processing techniques and system identification methods, provide useful information to investigate site and structure dynamic properties. In this report seismic response measurements from downhole array and adjacent bridge foundation sensors provided unique insights into the seismic response of a soil-foundation-structure system.

6.1 Strong Motion Data Analysis

At present, uncertainties remain regarding input ground motion and role of the foundation in bridge system analyses. The recorded seismic response at the Eureka geotechnical downhole array, and two nearby heavily instrumented bridges – the Samoa Channel Bridge and Eureka Channel Bridge continues to have the potential to provide valuable insights. Overview and highlights of the related conducted studies include:

(1) Sensors placed in the pile during the retrofit phase along with the adjacent subsurface geotechnical array allowed for comparisons of the site and foundation seismic responses.

(2) During the moderate shaking event (the 2010 Ferndale earthquake), soil nonlinearity was documented. In addition, the ground-foundation-bridge system for both the Samoa Channel Bridge and the Eureka Channel Bridge experienced a clear reduction in stiffness.

(3) For the Samoa Channel Bridge, the pile cap of Pier S-8 (at the center bent) is 16.7 m above the mudline. As such, much of the observed bridge deflections (both in the transverse and longitudinal directions) was emanating from movement of the pile group.

(4) Significant effects of SSI on the bridge structure may be assessed with the help of recorded strong motion data and identification techniques. The conducted studies attempt to provide a preliminary framework for such efforts.

Overall, the insights obtained from this study concerning observed behavior of a full-scale bridge and pile foundation during actual earthquake events are extremely valuable and contribute considerably to our current understanding of this important SSI mechanism. Further details and studies can be found in Wang (2015).

6.2 Numerical Modeling of Ground-Foundation-Structure system

A goal of this report is to characterize and identify the effects of foundation flexibility on the ground-foundation-bridge system by developing a simple reliable method to assess recorded earthquake motions. Identification techniques were employed to predict lateral stiffness of the pile groups at mid-span of two instrumented bridges. Procedures for identification of structure parameters (column stiffness, foundation stiffness and base spring values) are described and identification results are analyzed. Overall, the identified model parameters provide valuable insights into the structure-foundation-ground response mechanisms. Further details and studies can be found in Wang (2015).

References

Caltrans (1968). "As-Built Plans, Samoa Channel Bridge." California Department of Transportation, Sacramento, CA, personal communication.

Caltrans (2002a). "As-Built Plans, Earthquake Retrofit Project for Samoa Channel Bridge." California Department of Transportation, Sacramento, CA, personal communication.

Caltrans (2002b). "As-Built Plans, Earthquake Retrofit Project for Eureka Channel Bridge." California Department of Transportation, Sacramento, CA, personal communication.

Caltrans (2012). "Bridge Design Practice Manual." California Department of Transportation, Sacramento, CA.

Caltrans (2013). "Seismic Design Criteria Version 1.7." California Department of Transportation, Sacramento, CA.

Elgamal, A., Yang, Z., and Lu, J. (2006). "Cyclic1D: a computer program for seismic ground response." Report no. SSRP-06/05, Department of Structural Engineering, University of California, San Diego, La Jolla, CA.

Elgamal, A., Zeghal, M., Tang, H., and Stepp, J. (1995). "Lotung Downhole Array. I: Evaluation of Site Dynamic Properties." *Journal of Geotechnical Engineering*, 121(4), 350-362.

Elgamal, A. W., Zeghal, M., Parra, E., Gunturi, R., Tang, H. T., and Stepp, J. C. (1996). "Identification and modeling of earthquake ground response - I. Site amplification." *Soil Dynamics and Earthquake Engineering*, 15(8), 499-522.

EPRI (1993). "Guidelines for determining design basis ground motions." *Final Rep. No. TR-102293*, Electric Power Research Institute, Palo Alto, California.

Graizer, V., Shakal, A., and Hipley, P. "Recent data recorded from downhole geotechnical arrays." *Proc., SMIP2000 Seminar Proceedings*.

Huang, M., and Shakal, A. F. (1995). "CSMIP strong-motion instrumentation and records from the I10/215 interchange bridge near San Bernardino." *Earthquake Spectra*, 11(2), 193-215.

Malhotra, P. K., Huang, M. J., and Shakal, A. F. (1995). "Seismic interaction at separation joints of an instrumented concrete bridge." *Earthquake Engineering & Structural Dynamics*, 24(8), 1055-1067.

Seed, H. B., and Idriss, I. M. (1970). "Soil moduli and damping factors for dynamic response analyses." Earthquake Engineering Research Center, Report No. EERC 70-10, University of California, Berkeley, California.

Shamsabadi, A., Abazarsa, F., Ghahari, S., Nigbor, R., and Taciroglu, E. "Bridge Instrumentation: Needs, options, and consequences." *Proc., Istanbul Bridge Conference*.

Shantz, T. (2013). "Guidelines on foundation loading and deformation due to liquefaction induced lateral spreading." *California Department of Transportation, Sacramento, CA.*

Storesund, R., Dengler, L., Mahin, S., Collins, B. D., Hanshaw, M., Turner, F., and Welsh, K. (2010). "M6.5 Earthquake Offshore Northern California January 9, 2010." GEER Field Reconnaissance Summary.

Turek, M., Ventura, C. E., Dowling, J., Molnar, S., and Kaya, Y. (2014). "Ambient Vibration Testing of the Eureka-Samoa Channel Bridge." *Dynamics of Civil Structures, Volume 4*, Springer, 403-409.

Wang, N. (2015). "Three-Dimensional Modeling of Ground-Pile Systems and Bridge Foundations." Ph.D. Dissertation, University of California, San Diego, CA.

Wang, N., and Elgamal, A. "Bridge and adjacent downhole array responses during earthquakes at Eureka, California." *Proc., 110th International Conference on Urban Earthquake Engineering*.

Zeghal, M., Elgamal, A., Tang, H. T., and Stepp, J. C. (1995). "Lotung Downhole Array. II: Evaluation of Soil Nonlinear Properties." *Journal of Geotechnical Engineering*, 121(4), 363-378.